Biogeosciences Discuss., 12, 17393–17452, 2015
www.biogeosciences-discuss.net/12/17393/2015/
doi:10.5194/bgd-12-17393-2015

Biogeosciences
Discussions
Open Access

Water level, vegetation composition and plant productivity explain greenhouse gas fluxes in temperate cutover fens after inundation

M. Minke[1,5], J. Augustin[2], A. Burlo[3], T. Yarmashuk[4], H. Chuvashova[3], A. Thiele[5,6], A. Freibauer[1], V. Tikhonov[3], and M. Hoffmann[7]

[1]Thünen Institute of Climate – Smart Agriculture, Braunschweig, Germany
[2]Institute for Landscape Biogeochemistry, ZALF e.V., Müncheberg, Germany
[3]Scientific and Practical Centre of the National Academy of Sciences of Belarus for Biological Resources, Minsk, Belarus
[4]Institute for Nature Management of the National Academy of Sciences of Belarus, Minsk, Belarus
[5]Institute of Botany and Landscape Ecology, University Greifswald, Germany
[6]Michael Succow Foundation, Greifswald, Germany
[7]Institute of Soil Landscape Research, ZALF e.V., Müncheberg, Germany

Received: 10 September 2015 – Accepted: 12 October 2015 – Published: 29 October 2015

Correspondence to: M. Minke (merten.minke@ti.bund.de)

Published by Copernicus Publications on behalf of the European Geosciences Union.

Abstract

Rewetting of temperate continental cutover peatlands generally implies the creation of flooded areas, which are – dependent on water depth – colonized by helophytes such as *Eriophorum angustifolium*, *Carex* spp., *Typha latifolia* or *Phragmites australis*. Reeds of *Typha* and *Phragmites* are reported to be large sources of methane, but data on net CO_2 uptake are contradictory for *Typha* and rare for *Phragmites*. This paper describes the effect of vegetation, water level and nutrient conditions on greenhouse gas (GHG) emissions for representative vegetation types along water level gradients at two rewetted cutover fens (mesotrophic and eutrophic) in Belarus. Greenhouse emissions were measured with manual chambers in weekly to few – weekly intervals over a two years period and interpolated by modelling.

All sites had negligible nitrous oxide exchange rates. Most sites were carbon sinks and small GHG sources. Methane emissions were generally associated with net ecosystem CO_2 uptake. Small sedges were minor methane emitters and net CO_2 sinks, while *Phragmites australis* sites released large amounts of methane and sequestered very much CO_2. Variability of both fluxes increased with site productivity. Floating mats composed of *Carex* tussocks and *Typha latifolia* were a source for both methane and CO_2. We conclude that shallow, stable flooding is a better measure to arrive at low GHG emissions than deep flooding, and that the risk of high GHG emissions consequent on rewetting is larger for eutrophic than for mesotrophic peatlands.

1 Introduction

Cutover peatlands represent about ten percent of all drained peatlands outside the tropics with the main share in the Nordic countries and Eastern Europe (Joosten and Clarke, 2002). Since the 1990s restoration of cutaways was conducted especially in Canada, Finland, Sweden and Ireland. Similar projects in Eastern Europe started later, but already cover vast areas. 42 000 ha of degraded peatlands were restored in Belarus since 2007 and about 80 000 ha since 2010 in the European part of Russia, aiming to decrease GHG emissions from microbial peat oxidation and peat fire incidents (Tanneberger and Wichtmann, 2011; Wetlands International, 2015).

A large proportion of the peatlands that have been rewetted or are available for rewetting in Russia and Belarus are abandoned cutover fens (Minayeva et al., 2009; Tanovitskaya and Kozulin, 2011). Rewetting of such sites creates a mosaic of wet and flooded zones and elevated drier parts, and results in rapid vegetation changes (Kozulin et al., 2010; Thiele et al., 2011). At sites with the water level close to surface species like *Eriophorum angustifolium*, *Carex vesicaria* and *Lythrum salicaria* establish within few years, or, under more nutrient rich conditions, *Calamagrostis canescens*, *Lysimachia thyrsiflora*, *Carex elata* and *Salix*. At flooded areas with standing water depths of more than 20 cm mainly *Phragmites australis* emerges, whereas water levels above 30 cm in the medium term only result in the establishment of submerse and floating plants (Kozulin et al., 2010; Thiele et al., 2011).

Studies from rewetted cutover boreal peatlands and temperate bogs show that methane and carbon dioxide emissions are strongly related to vegetation, water level and nutrient conditions (Tuittila et al., 1999, 2000; Drösler, 2005; Yli-Petäys et al., 2007; Soini et al., 2010; Samaritani et al., 2011; Strack and Zuback, 2013; Wilson et al., 2013; Beyer et al., 2015). Interannual variability of meteorological conditions, water levels and plant productivity can substantially affect annual GHG emissions from pristine and restored peatlands (Wilson et al., 2013; Günther et al., 2014; Helfter et al., 2015). For rewetting it is frequently recommended to raise the water level throughout the year to close to the surface and to avoid inundation in order to promote the establishment of peat forming vegetation and to prevent high methane emissions (Drösler et al., 2008; Couwenberg et al., 2008, 2011; Joosten et al., 2012). Such conditions have been proven optimal for bog restoration (Beyer et al., 2015), but their feasibility for fens has been questioned (Koebsch et al., 2013; Zak et al., 2015).

So far, complete GHG balances are not available for rewetted temperate cutover fens. Such fens differ from those in the above cited studies in particular by the massive establishment in shallow water of *Typha* and *Phragmites australis*, i.e. of species that are potentially strong sources of methane (Kim et al., 1998; Brix et al., 2001; Whiting and Chanton, 2001; Kankaala et al., 2004; Hendriks et al., 2007; Chu et al., 2015; Knox et al., 2015; Strachan et al., 2015). Whereas earlier studies indicate that the radiative forcing of such methane emissions may be compensated for by the simultaneous very strong net CO_2 uptake (Brix et al., 2001; Whiting and Chanton, 2001), recent observations described *Typha* dominated wetlands as often only weak CO_2 sinks (Rocha and Goulden, 2008; Chu et al., 2015; Strachan et al., 2015; but cf. Knox et al., 2015). *Phragmites australis*, the more abundant species in European rewetted cutover fens is according to Brix et al. (2001) a potentially stronger net CO_2 sink, but no annual CO_2 exchange rates have yet been published from permanently inundated *Phragmites australis* wetland sites.

To fill this knowledge gap we measured the CO_2, CH_4, and N_2O emissions from *Phragmites australis* communities and other representative vegetation types along water level gradients in two rewetted cutover fens with different nutrient conditions in Belarus. Our objectives were: (i) to assess GHG emissions from rewetted temperate cutover fens recolonized by wetland plants (ii) to analyse the effect of water level, vegetation and nutrient conditions on GHG exchange, and (iii) to estimate the inter-annual and spatial variability of GHG emissions.

2 Materials and methods

2.1 Study sites

Greenhouse gas fluxes were measured at two sites in Belarus with a temperate continental climate with fully humid conditions and warm summers (Dfb after Köppen, 1936; cf. Kottek et al., 2006). Both sites have been subject to peat extraction, but differ with respect to time since rewetting, water depth, peat characteristics, vegetation, and regional climate.

“Barcianicha” (54.10° N; 26.29° E) is located in central Belarus on an alluvial plain between the rivers Al’šanka and Zahodniaia (“Western”) Biarėzina and predominantly fed by groundwater discharge (Maksimenkov et al., 2006). In 1990 about 190 ha of Barcianicha were drained and from 1992 to 1995 peat was extracted by milling over an area of 150 ha to a remaining peat depth of about 80 cm. After abandonment ditches were closed with earth dams and water level was raised over 60 % of the area, allowing wetland species like *Phragmites australis*, *Carex rostrata* and *Eriophorum angustifolium* to establish despite strong water level amplitudes between summer and winter (Maksimenkov et al., 2006). In 2007 weirs and overflow dams were built, which stabilized water levels. In 2010 most of the area had water levels at or slightly above the surface throughout the year. Vast reeds, dominated by *Phragmites australis* of up to two metres height, covered the area. Three GHG monitoring sites were installed along a water level gradient, including an *Eriophorum angustifolium*–*Carex rostrata* site (further indicated as BA *Eriophorum*–*Carex*), a *Carex rostrata*–*Equisetum fluviatile* site (BA *Carex*–*Equisetum*) 15 m further and a *Phragmites australis*–*Carex rostrata* site (BA *Phragmites*–*Carex*) after another 30 m (Table 2).

The second peatland, “Giel’čykaŭ Kašyl’” (52.38° N; 25.21° E), forms part of the “Bierastaviec” fen and is situated on the left bank of Jasiel’da river. It belongs to the Ramsar site “Sporaŭski zakaznik” and was drained in 1975 (Kadastrovyj spravochnik, 1979). After peat extraction more than one metre of peat remained and grassland was established. But as the area proved to be unsuited for hay production, the pumping station was turned off in 1985 and the area was flooded by the Jasiel’da, which is connected with Giel’čykaŭ Kašyl’ by a 300 m long channel. During the vegetation period the area receives additional water that is pumped out of an adjacent drained fen. *Phragmites australis* of three metres height dominates the area, which is flooded up to one metre above the surface. A 30–80 m wide swampy terrestrialization zone along the edges is formed by *Typha latifolia*, *T. angustifolia*, and tussocks of *Carex elata* and *C. vesicaria* floating on up to one metre of water. GHG monitoring was performed in the terrestrialization zone at two sites: a *Carex elata*–*Lysimachia thyrsiflora* site (GK

Carex–Lysimachia), and a *Typha latifolia–Hydrocharis morsus–ranae* site (GK *Typha–Hydrocharis*; Table 2), both close to each other. The third *Phragmites australis–Lemna trisulca* site (GK *Phragmites–Lemna*) was situated 20 m from the first two sites in the deeper inundated main area, separated from the terrestrialization zone by a flooded ditch.

2.2 Site characteristics

Peat depth, stratigraphy and degree of decomposition after Von Post (AG Boden, 2005) were assessed visually for each site using a chamber corer (50 cm long, 5 cm diameter). One mixed surface peat sample (0–5 cm) from each plot was analysed for total carbon (C) and total N (Vario EL III, Germany), and three samples per plot for pH (Hanna Combo HI 98130, calibrated with 7.01 and 4.01 buffer solution, stored in KCl solution, HANNA instruments, USA). After the study, above ground biomass was harvested from all plots (Barcianicha, 29 October 2012; Giel'čykaŭ Kašyl', 11 September 2012), oven dried at 60 °C till weight constancy, and three mixed samples per plot were analysed for total C and N.

Vegetation cover of the 70 cm × 70 cm plots was assessed in coverage classes after Peet et al. (1998). Nomenclature for vascular plants and mosses follows Rothmaler (2002), and Abramov and Volkova (1998), respectively.

Water levels were measured continuously (daily averages stored) with Mini Diver data loggers (Eigenbrodt, Germany), installed in perforated tubes (inner diameter 46 mm). One Diver was situated next to BA *Carex–Equisetum* in Barcianicha, and another in the middle between the terrestrialization zone sites and GK *Phragmites–Lemna* in Giel'čykaŭ Kašyl'. Manual water level measurements were conducted at each site in every second to third week. To derive mean daily water levels relative to ground surface for every plot we first calculated continuous water level time series for every site by linear regression between automatically and manually measured water levels and than corrected for the distances between surface of plots and top of water level tubes. This did not work for GK *Typha–Hydrocharis* and GK *Carex–Lysimachia* because of strong peat oscillation. Photographic documentation (monthly during vegetation season, one time per winter) was used here instead to reconstruct relative water levels for linear regression with Diver records.

2.3 Measurement of greenhouse gas exchange

In order to account for typical small-scale differences between vegetation types we applied a manual chamber approach to measure greenhouse gas exchange. Each of the six GHG measurement sites was equipped with three plastic collars of 70 cm × 70 cm, established in a row about 40 cm apart from each other. Collars were inserted 15 cm deep into the peat at Barcianicha. At Giel’čykaŭ Kašyl’ because of the high water level, collars were fixed on tubes orthogonally inserted in the peat and anchored in the underlying sand. Measurements were conducted from pre-installed boardwalks from August 2010 to August 2012.

CO_2 exchange was measured with air mixed (fan) transparent chambers (TF) made of plexiglas (inner size 72.5 cm × 72.5 cm × 51.2 cm, 88 % light transmission, ice packs for cooling, Drösler, 2005) and same sized, air mixed opaque chambers with fan (DF) made of grey ABS plastic covered with a white film. Opaque and transparent extensions with open tops were used to enlarge the chambers to accommodate for tall plants. Chambers and extensions were sealed airtight by closed cell rubber tubes attached to the bottom rims (Drösler, 2005). Carbon dioxide concentrations were measured continuously by circulating air in a closed loop between the chamber and an infrared gas analyser (LI-820, LI-COR Biosciences, USA) and recorded every five seconds by a data logger (CR200 or CR1000, Campbell Scientific, USA). Simultaneously, air temperature inside and outside the chamber, and PAR were recorded automatically (“109” temperature probes protected by radiation sheets, SKP215, Campbell Scientific, USA), while soil temperatures were measured manually in 2, 5, and 10 cm depth once per chamber measurement with Pro-DigiTemp insertion thermometers (Carl Roth, Germany). During a measuring campaign (a bright or hardly cloudy day to capture the complete PAR range from zero to solar noon) eight to ten transparent chamber measurements of two to three minutes were carried out on each plot from dawn until late afternoon. Measurements were equally distributed over the daily range of PAR to determine light response of gross primary production (GPP). A similar number of opaque chamber measurements of 3–5 min were performed over the same period to capture the temperature response of ecosystem respiration (R_{eco}). Measurement campaigns were repeated every third to fourth week to account for seasonal changes in water table depth and plant development.

CH_4 and N_2O fluxes were measured once every second to third week during the snow free period and monthly during winter using non-air mixed opaque chambers (D), of the same material as DF, but shaped as a truncated pyramid (inner size at bottom 72.5 cm × 72.5 cm, inner size at top 62.5 cm × 62.5 cm, height 51.2 cm). Four to five air samples were taken from the chamber headspace during a 15–20 min enclosure and subsequently analysed in the laboratory with a gas chromatograph (Chromatec-Cristal 5000.2, Chromatec, Russia), using an electron capture detector (ECD) for analysing N_2O and a flame ionization detector (FID) for CH_4, and an auto-sampler (Loftfield, Germany). Air and soil temperatures were measured with Pro-DigiTemp insertion thermometers. From August 2010 to August 2012 a total of 36 CH_4 and N_2O as well as 26 CO_2-measuring campaigns were carried out at every site.

Diurnal CH_4 emission dynamics and the effect of chamber transparency and headspace mixing were additionally studied at one plot per site by frequent CH_4 measurements for one to two summer days, using alternately two (DF and TF) or three (D, DF, and TF) chamber types (for details cf. Minke et al., 2014).

Parameters for the development of flux models were recorded on site during GHG-measuring campaigns, and monitored continuously by nearby climate stations (BA: Višnieva, 5.6 km NW of Barcianicha, and GK: Z'dzitava, 6.3 km NE of Giel'čykaŭ Kašyl'). At the stations soil temperatures in 2 and 5 cm depth, and air temperature 20 cm above surface were measured with "109" temperature probes (Campbell Scientific, USA). Photosynthetically active radiation (PAR) was monitored using a SKP215 Quantum Sensor, precipitation with 52202 Raingauge Heated European, atmospheric pressure with CS100 Setra Barometric Sensor, and all data were recorded half-hourly with CR200 data loggers (all devices from Campbell Scientific, USA). Regression between site and climate station temperature data was subsequently applied to derive continuous half-hourly time series for each site. Due to technical problems with the rain gauges precipitation data were received from Gidrometcentr, Belarus, from the weather stations in Valožyn (15 km E of Barcianicha) and Pružany (54 km WNW of Gieľčykaŭ Kašyl'). Data from both weather stations of Gidrometcentr were also used to calculate 30 year (1979–2008) monthly averages of air temperature and precipitation.

2.4 Calculation of flux rates, annual emission models and uncertainty

2.4.1 Carbon dioxide

The net ecosystem exchange (NEE, the CO_2 flux between the ecosystem and the atmosphere) is the balance between CO_2 inputs to the ecosystem by gross primary production (GPP) and CO_2 losses by ecosystem respiration (R_{eco}; Alm et al., 1997; Chapin et al., 2002). A positive sign refers to a flux from the ecosystem to the atmosphere, a negative sign to an ecosystem sink (cf. Falge et al., 2001). Annual NEE rates were modelled for each plot separately based on the plot – and campaign specific relationships between R_{eco} and temperature, and between GPP and PAR.

To account for possible impacts of the calculation routine and underlying assumptions on the result we used the R script Version 1.4 of Hoffmann et al. (2015) ("APPROACH ONE") and the R script of Leiber-Sauheitl et al. (2014) ("APPROACH TWO"). Both approaches base on Drösler (2005), but differ with respect to flux calculation, reference temperature, GPP model and importance of the significance of the model fits, as described in the following paragraphs.

Calculation of measured CO_2 flux rates

Measured CO_2 flux rates were calculated in both approaches by linear regression. Measurements were discarded if PAR differed > ±10 % (transparent chambers) and chamber temperature > ±0.75 K (transparent and opaque chambers) from the mean of the selected flux calculation interval. APPROACH ONE applied a moving window of variable time to adjust the starting point and length of the regression sequence to the regression quality and selected the optimal flux length in a second step, based on the minimum Akaike Information Criterion (AIC) of its fit to the R_{eco} and the GPP functions, respectively. APPROACH TWO used a moving window of constant length (one minute for all, but two minutes for opaque flux measurements at *Phragmites australis* plots because of large chamber volumes and slow concentration changes) to select the regression sequence with maximum R^2 and minimum variance. If maximum R^2 resulted in different fluxes than minimum variance (46 % of all flux measurements) the mean of both was used as flux estimate.

Modelling of half-hourly CO_2 exchange rates

Both approaches fitted R_{eco} flux data to site temperatures for each plot and campaign by the Lloyd and Taylor (1994) equation (Eq. 1).

$$R_{eco} = R_{ref} \times \exp\left[E_0 \times \left(\frac{1}{T_{ref} - T_0} - \frac{1}{T - T_0}\right)\right] \quad (1)$$

R_{eco} = ecosystem respiration ($mg\,CO_2{-}C\,m^{-2}\,h^{-1}$), $R_{ref} = R_{eco}$ at reference temperature ($mg\,CO_2{-}C\,m^{-2}\,h^{-1}$), E_0 = activation energy like parameter (K), T_{ref} = reference temperature (283.15 K), T_0 = temperature constant for the start of biological processes: (227.13 K), T = soil or air temperature during measurement of best fit with the dataset (K).

APPROACH ONE fitted Eq. (1) to calculated R_{eco} flux rates separately for air temperature and soil temperatures and selected the final R_{eco} parameter pairs out of all significant ($p \leq 0.1$) sets based on the lowest AIC. If parameterization was not significant or failed, or if the daily temperature amplitude was below 3 K, the average CO_2 flux of the measurement campaign was used. APPROACH TWO calculated one R_{eco} fit per plot and campaign in relation to air temperatures, because only one flux was estimated per measurement. If parameterization was impossible or the temperature ranged below 2 K, the mean campaign R_{eco} flux was used.

In a second step GPP fluxes were determined by subtracting modelled R_{eco} fluxes from timely corresponding, measured NEE flux rates. APPROACH ONE fitted a rectangular hyperbola equation (Michaelis-Menten, 1913; Eq. 2) to the relation between PAR and GPP flux rates to calibrate GPP parameter sets of α (initial slope of the curve; light use efficiency) and GP_{max} (rate of carbon fixation for infinite PAR).

$$\mathrm{GPP} = \frac{\alpha \times \mathrm{PAR} \times \mathrm{GP_{max}}}{\alpha \times \mathrm{PAR} + \mathrm{GP_{max}}} \tag{2}$$

GPP parameter pairs with lowest AIC were selected from each campaign out of all significant regression parameters ($p \leq 0.1$). If the parameter estimation failed, a non-rectangular hyperbolic equation was fitted to the data (Gilmanov et al., 2007). If this failed, too, an average parameter approach was used. APPROACH TWO applied the modified Michaelis-Menten model of Falge et al. (2001; Eq. 3) and calculated GP2000 instead of GP_{max}, i.e. the rate of carbon fixation at PAR of 2000 $\mu mol\,m^{-2}\,s^{-1}$. Campaigns for which no GPP fit was found were skipped.

$$\mathrm{GPP} = \frac{\alpha \times \mathrm{PAR} \times \mathrm{GP2000}}{\mathrm{GP2000} + \alpha \times \mathrm{PAR} - \frac{\mathrm{GP2000}}{2000} \times \mathrm{PAR}} \tag{3}$$

Based on the GPP parameter pairs and continuously monitored PAR data, GPP was modelled by both approaches for each plot at a temporal resolution of 30 min. NEE was subsequently calculated as the difference between GPP and R_{eco}.

As both approaches used very similar functions and produced similar results we focus on APPROACH ONE for the presentation and discussion of the modelled CO_2 time series. Annual budgets are presented as the mean of both approaches.

Uncertainty, accuracy, and variability

Model performance for the interpolation between the measurement campaigns was estimated for APPROACH ONE by leave-one-out cross-validation. Stepwise one measuring campaign was left out after the other and the model calculated with the remaining campaigns, comparing the modelled R_{eco} and NEE fluxes with the measured ones at the left out campaign. Model performance was assessed by the Nash–Sutcliffe efficiency (NSE, Moriasi et al., 2007).

The random error of the annual CO_2 balances was calculated for APPROACH ONE using the R-script Version 1.1 of Hoffmann et al. (2015). From every campaign specific confidence interval ($p = 0.01$) created by bootstrapping for the temperature models, R_{eco} and GPP parameter pairs, 100 samples were randomly taken to compute R_{eco}, GPP, and NEE models. The calculated 90 % confidence intervals of annual R_{eco}, GPP and NEE fluxes represent the uncertainty of the measuring campaigns, but not of the interpolation.

Uncertainties of annual emissions were estimated as 50 % of the difference between annual sums of both approaches plus the annual random error calculated for APPROACH ONE.

Inter-annual variability of annual NEE fluxes was calculated as the absolute differences between annual plot emissions and two years plot mean. Small scale spatial variability was calculated as the absolute differences between annual plot emissions and annual site emissions.

2.4.2 Methane

Calculation of methane fluxes

Methane fluxes were calculated with the R package “flux 0.2–1” (Jurasinski et al., 2012) using linear regression. Outliers were eliminated for normalized root mean square error

(NRMSE) ≥ 0.2, what was the case in 168 out of a total of 645 methane flux measurements from all campaigns. Fluxes were accepted if NRMSE < 0.4, $R^2 \geq 0.8$ and $n \geq 3$.

Modelling of methane emissions

A nonlinear regression model for calculation of daily methane fluxes was developed in two steps. First, the relation between environmental factors (air temperature, soil temperature, water level, air pressure, PAR, GPP, R_eco, NEE) and measured CH_4 fluxes was tested for each plot using non-parametric Spearman's correlation to identify the strongest driving parameter. Second, a nonlinear regression model was selected that best reflects the relation between methane emissions and the driver.

The strongest Spearman's ρ correlations were found between methane fluxes and instantaneous on site soil temperature (median ρ for two years and all 18 plots = 0.85, $n = 36$), followed by half-hourly and daily R_eco (both 0.83), half-hourly GPP (−0.80; both modelled with APPROACH ONE), and on site air temperature (0.75). Mean daily site specific soil temperatures, calculated by linear regression between site measurements and climate station data, also correlated well with methane fluxes (median ρ per plot and year = 0.85) and had a strong covariance with other factors. Water level did not correlate significantly with methane emissions at any plot, possibly because it was always close to or above the surface. Therefore mean daily soil temperature was chosen as the single driving factor for modelling methane emission.

The temperature dependency of methane production and emission was previously described by the Arrhenius function or its logarithmic form (Conrad et al., 1987; Schütz et al., 1990; Daulat and Clymo, 1998; Kim et al., 1998)

$$F = A \times e^{\frac{-E}{R \times T}} \tag{4}$$

F = flux rate of CH_4 ($\text{mg}\,CH_4-\text{C}\,\text{m}^{-2}\,\text{h}^{-1}$), A = Arrhenius parameter ($\text{mg}\,CH_4-\text{C}\,\text{m}^{-2}\,\text{h}^{-1}$), E = apparent activation energy ($\text{J}\,\text{mol}^{-1}$), R = gas constant ($8.314\,\text{J}\,\text{mol}^{-1}\,\text{K}^{-1}$), T = soil temperature (K).

Also an exponential function or its logarithmic form has been widely applied to calculate methane emission in relation to temperature (Dise and Gorham, 1993; Saarnio et al., 1997; Kettunen et al., 2000; Tuittila et al., 2000; Laine et al., 2007; Rinne et al., 2007; Wilson et al., 2009):

$$F = a \times e^{b \times T} \tag{5}$$

F = flux rate of CH_4 ($mg\,CH_4{-}C\,m^{-2}\,h^{-1}$), a = flux rate at $T = 0\,^{\circ}C$ ($mg\,CH_4{-}C\,m^{-2}\,h^{-1}$), b = coefficient ($^{\circ}C^{-1}$), T = soil temperature ($^{\circ}C$).

The third function we tested was the equation developed by Lloyd and Taylor (1994) for soil respiration (Eq. 1, Sect. 2.4.1).

We used the AIC to select from Eqs. (1), (4), and (5) the one that best fitted to our data set. The differences were small but the AIC of the Lloyd and Taylor function (Eq. 1) was the smallest for 33 out of 36 fits (fits for 2 years and 18 plots) and was therefore chosen to model methane emissions for all plots and years.

Uncertainty, accuracy, and variability

Model performance was tested by leave-one-out cross-validation.

Errors of modelled annual methane emissions were calculated using Monte Carlo simulation in four steps. First, the linear regression between soil temperatures at site and climate station was performed 1000 times with bootstrapped re-sampling of site temperature data points. Second, a set of 1000 normally distributed flux values was generated for every flux measurement based on mean and standard deviation. Third, each of the soil temperature data set was paired with one of the flux data sets and the residuals of the resulting 1000 Lloyd and Taylor fits (Eq. 1) were bootstrapped 1000 times. Finally, 1000 Lloyd and Taylor fits were randomly selected, paired with the soil temperature data set and 1000 methane models were calculated. As the CH_4 model fit includes all data of a year, the 90 % confidence interval does to some extent also account for the interpolation between measuring days.

Inter-annual and small scale spatial variability of annual methane emissions was calculated in the same way as of NEE (2.4.1).

2.4.3 Nitrous oxide

Flux rates

Nitrous oxide flux rates and their standard deviations were calculated with linear regression using the same air samples as accepted for CH_4 flux calculation.

Annual emissions

Measured N_2O fluxes were linearly interpolated for annual emission estimates.

Uncertainty

Based on flux mean and standard deviation 1000 normally distributed values of each flux were generated and linearly interpolated. The 90 % confidence intervals calculated from the resulting 1000 annual emission estimates represent the uncertainty of the measured fluxes.

2.5 Statistical analyses

Correlations between annual balances of CH_4 and CO_2 with site factors were tested using the non-parametric Spearman's ρ.

Differences of daytime methane fluxes among chamber types were analysed using either the Mann–Whitney test or the Kruskal–Wallis test with the post-hoc nonparametric Tukey-type multiple comparison procedure developed by Nemenyi (Zar, 1999).

3 Results

3.1 Site conditions

Mean annual temperature at Barcianicha during the first year (15 August 2010–14 August 2011) was 6.5 °C which corresponds to the long term mean (6.4 °C, 1979–2008). The second year (15 August 2011–14 August 2012) was slightly warmer (6.9 °C). Annual precipitation in the first year was, due to heavy summer rains (Fig. 1a), higher compared to the long-term mean (740 vs. 665 mm), and in the second year lower (633 mm). Mean daily air temperatures were above 5 °C for 209 days and below 0 °C for 97 days during the first year, but only for 195 and 73 days, respectively, during the second year.

At Giel'čykaŭ Kašyl' long-term mean annual temperatures were generally higher and precipitation lower (7.3 °C and 594, respectively, 1979–2008) compared to Barcianicha. The deviations of both years from the long-term mean, however, were in the same direction: the first year annual temperature was the same and precipitation larger (804 mm) as compared to the long-term mean, while the second year was warmer (7.9 °C) and drier (500 mm). Heavy rains occurred in September and November 2010 and August 2011, while September and October 2011 and July 2012 almost suffered from water deficits (Fig. 1b). The warm period (> 5 °C) at Giel'čykaŭ Kašyl' was longer in both years (222 and 210 days) as compared to Barcianicha and the frost period shorter (90 and 66 days).

Annual water levels relative to the surface at Barcianicha were highest at BA *Phragmites–Carex* (13 to 16 cm above surface), slightly lower at BA *Carex–Equisetum* and just below surface at BA *Eriophorum–Carex* (Table 1). Differences among plots within sites were small. Annual values for both years were the same. Summer and winter median water levels were very similar, despite of temporal fluctuations of up to 18 cm (Fig. 3, Table 1).

Water tables at GK *Phragmites–Lemna* (Giel'čykaŭ Kašyl') were about one metre above surface in the first year, and dropped by 30 cm in the second year (Table 1). At the close by sites GK *Typha–Hydrocharis* and GK *Carex–Lysimachia* water levels were only up to 13 cm above the surface and the drop from the first to the second year was small, both because of the oscillating peat surface. Summer water levels were lower than winter levels, but never dropped significantly below surface (Table 1, Fig. 4). Differences of annual water levels among plots within sites at Giel'čykaŭ Kašyl' were larger as compared to Barcianicha, with a maximum of 11 cm at GK *Phragmites–Lemna*.

Most of the residual peat at both peatlands was very slightly to moderately decomposed radicel peat (Table 1). Barcianicha had about 40 cm below surface 27 to 76 cm thick layers of brown moss peat, while for Giel'čykaŭ Kašyl' notable amounts of *Phragmites* macrofossils were found in the upper 100 to 140 cm of the profile. Surface peat was eutrophic and acid at both study sites, but less decomposed at Barcianicha as compared to Giel'čykaŭ Kašyl' (Table 1).

Vegetation was homogeneous within sites types at Barcianicha and did only slightly vary between years (Table 2). BA *Eriophorum–Carex* was dominated by *Eriophorum angustifolium*, BA *Carex–Equisetum* by *Carex rostrata* and BA *Phragmites–Carex* by *Phragmites australis*. Nutrient conditions as indicated by vegetation were mesotrophic at Barcianicha (Koska et al., 2001).

Differences in species cover among plots and years were also small for GK *Phragmites–Lemna* at Giel'čykaŭ Kašyl' (Table 2). The sites GK *Carex–Lysimachia* and GK *Typha–Hydrocharis* constituted a strongly interweaved fine mosaic of sedge tussocks and cattail and shared many species. Vegetation indicated eutrophic conditions for Giel'čykaŭ Kašyl' (Koska et al., 2001).

Above ground biomass harvested in autumn 2012 at Barcianicha (Table 1) was largest for BA *Phragmites–Carex* (221–379 $\mathrm{g\,C\,m^{-2}}$), lower for BA *Eriophorum–Carex* (97–156 $\mathrm{g\,C\,m^{-2}}$) and smallest for BA *Carex–Equisetum* (31–73 $\mathrm{g\,C\,m^{-2}}$). Biomass harvests of GK *Typha-Hydrocharis* and GK *Carex-Lysimachia* were similar to BA *Phragmites–Carex*, but that of GK *Phragmites–Lemna* were two times larger (502–725 $\mathrm{g\,C\,m^{-2}}$, Table 1). Higher biomass production of *Phragmites australis* at Giel'čykaŭ Kašyl' compared to Barcianicha is another indicator of different nutrient status in both peatlands, probably resulting from different water supply (river and grassland drainage water for GK, groundwater for BA) and different land use history (after peat extraction temporary grassland before rewetting of GK, rewetting directly after peat extraction of BA).

3.2 Carbon dioxide emissions

Model performance tested for APPROACH ONE was good for both years and all site types and plots. Cross-validation resulted in a median NSE of 0.78 (range from 0.38 to 0.90) for the R_{eco} models and of 0.76 (0.21 to 0.91) for the NEE models.

Annual R_{eco} fluxes varied significantly among the sites studied at Barcianicha. Site-wise averaged R_{eco} for the first and second year were 614 and 706 $\mathrm{g\,CO_2-C\,m^{-2}\,yr^{-1}}$ from BA *Phragmites–Carex*, 364 and 406 $\mathrm{g\,CO_2-C\,m^{-2}\,yr^{-1}}$ from BA *Eriophorum–Carex*, 232 and 327 $\mathrm{g\,CO_2-C\,m^{-2}\,yr^{-1}}$ from BA *Carex–Equisetum* (Table 3). At Barcianicha R_{eco} increased from the first to the second year for all sites, but most significantly for BA *Carex–Equisetum* as indicated by lacking overlap of confidence intervals between years. Within site variability was small for BA *Eriophorum–Carex* and BA *Carex–Equisetum*, and more pronounced for BA *Phragmites–Carex* (Fig. 5, Table S2 in the Supplement). Also the timelines were nearly identical among plots of BA *Eriophorum–Carex* and BA *Carex–Equisetum* while daily R_{eco} emissions from BA *Phragmites–Carex* during the summers were lower from plot one than from the other plots (Fig. 3). With respect to annual GPP fluxes the sites of Barcianicha followed the same order as for R_{eco}, but the annual GPP sink was smaller in the second as compared to the first year (Table 3). GPP fluxes from BA *Phragmites–Carex* were −1141 and −1035 $\mathrm{g\,CO_2-C\,m^{-2}\,yr^{-1}}$ in the first and second year, respectively, but only −449 and −413 $\mathrm{g\,CO_2-C\,m^{-2}\,yr^{-1}}$ from BA *Eriophorum–Carex*, and −320 and −302 $\mathrm{g\,CO_2-C\,m^{-2}\,yr^{-1}}$ from BA *Carex–Equisetum*. Daily and annual variability of GPP among plots within sites was more pronounced than of R_{eco} (Figs. 3 and 5). All site of Barcianicha were net $\mathrm{CO_2}$ sinks in the first year (Fig. 5). NEE fluxes from BA *Phragmites–Carex* were $-528\,\mathrm{g\,CO_2-C\,m^{-2}\,yr^{-1}}$ and lower from BA *Eriophorum–Carex* and BA *Carex–Equisetum* (-86 and $-88\,\mathrm{g\,CO_2-C\,m^{-2}\,yr^{-1}}$, respectively; Table 3). In the second year, resulting from increased R_{eco} and decreased GPP, NEE was lower from BA *Phragmites–Carex* ($-329\,\mathrm{g\,CO_2-C\,m^{-2}\,yr^{-1}}$) and BA *Eriophorum–Carex* ($-7\,\mathrm{g\,CO_2-C\,m^{-2}\,yr^{-1}}$) and BA *Carex–Equisetum* became a small net CO_2 source ($24\,\mathrm{g\,CO_2-C\,m^{-2}\,yr^{-1}}$; Table 3). Inter-annual variability of NEE fluxes was $110\pm113\,\mathrm{g\,CO_2-C\,m^{-2}\,yr^{-1}}$ for BA *Phragmites–Carex*, $39\pm12\,\mathrm{g\,CO_2-C\,m^{-2}\,yr^{-1}}$ for BA *Eriophorum–Carex* and $56\pm8\,\mathrm{g\,CO_2-C\,m^{-2}\,yr^{-1}}$ for BA *Carex–Equisetum* (Table 4, Fig. 5). Small scale variability of NEE was similar to inter-annual variability for BA *Phragmites–Carex* ($125\pm140\,\mathrm{g\,CO_2-C\,m^{-2}\,yr^{-1}}$) but smaller for BA *Eriophorum–Carex* and BA *Carex–Equisetum* (16 ± 13 and $9\pm5\,\mathrm{g\,CO_2-C\,m^{-2}\,yr^{-1}}$, respectively).

Annual R_{eco} fluxes from Giel'čykaŭ Kašyl' sites were higher than from Barcianicha. They were largest in both years from GK *Carex–Lysimachia* (1105 and $1270\,\mathrm{g\,CO_2-C\,m^{-2}\,yr^{-1}}$), followed by GK *Phragmites–Lemna* (936 and $1092\,\mathrm{g\,CO_2-C\,m^{-2}\,yr^{-1}}$) and GK *Typha–Hydrocharis* (921 and $973\,\mathrm{g\,CO_2-C\,m^{-2}\,yr^{-1}}$; Table 3). Differences between sites were less clear than in Barcianicha and confidence intervals of GK *Phragmites–Lemna* overlapped with both other sites. Annual R_{eco} fluxes from GK *Carex–Lysimachia* significantly increased from the first to the second year. The increase was similarly strong though not significant for GK *Phragmites–Lemna* but small for GK *Typha–Hydrocharis*. There was considerable variability of daily and annual R_{eco} emissions among plots within all sites of Giel'čykaŭ Kašyl' (Figs. 4 and 5, Table S2 in the Supplement). Annual GPP fluxes at Giel'čykaŭ Kašyl' were generally higher than at Barcianicha but the order of sites with respect to GPP fluxes did not follow that of R_{eco} (Table 3). GK *Phragmites–Lemna* had with $-1547\,\mathrm{g\,CO_2-C\,m^{-2}\,yr^{-1}}$ in the first and $-2267\,\mathrm{g\,CO_2-C\,m^{-2}\,yr^{-1}}$ in the second year the largest annual GPP rates. GPP fluxes of GK *Carex–Lysimachia* and GK *Typha–Hydrocharis* were lower, but also increased from the first to the second year (from -940 to -1054 and from -771 to $-1086\,\mathrm{g\,CO_2-C\,m^{-2}\,yr^{-1}}$ for GK *Carex–Lysimachia* and GK *Typha–Hydrocharis*, respectively). As for Barcianicha, daily and annual within sites variability of GPP was stronger than of R_{eco} (Figs. 4 and 5). The largest net CO_2 sink among all studied sites was GK *Phragmites–Lemna* (Table 3). NEE of this site was $-611\,g\,CO_2-C\,m^{-2}\,yr^{-1}$ in the first and $-1175\,g\,CO_2-C\,m^{-2}\,yr^{-1}$ in the second year. GK *Typha–Hydrocharis* varied between net source of $151\,g\,CO_2-C\,m^{-2}\,yr^{-1}$ in the first year and sink of $-113\,g\,CO_2-C\,m^{-2}\,yr^{-1}$ in the second year. GK *Carex–Lysimachia* was a net CO_2 emitter in both years (166 and $216\,g\,CO_2-C\,m^{-2}\,yr^{-1}$). NEE varied considerably between the three plots of each site at Giel'čykaŭ Kašyl' (Fig. 5, Table S2) and confidence intervals on the site level were accordingly wide (Table 3). Small scale spatial NEE variability of GK *Phragmites–Lemna* was $187\pm153\,g\,CO_2-C\,m^{-2}\,yr^{-1}$ (Table 4). It was also high for GK *Typha–Hydrocharis* and GK *Carex–Lysimachia* (121 ± 66 and $95\pm73\,g\,CO_2-C\,m^{-2}\,yr^{-1}$), despite of much smaller NEE. Inter-annual NEE variability of GK *Phragmites–Lemna* was higher than spatial variability ($282\pm177\,g\,CO_2-C\,m^{-2}\,yr^{-1}$). It was similar to spatial NEE variability for GK *Typha–Hydrocharis* and GK *Carex–Lysimachia* (132 ± 64 and $74\pm56\,g\,CO_2-C\,m^{-2}\,yr^{-1}$).

3.3 Methane emissions

3.3.1 Diurnal variability of methane emissions and impact of chamber types

Environmental conditions (inside air temperature and relative humidity, outside PAR) during the measurement campaigns of the diurnal methane patterns were comparable among chamber types, with the exception of BA *Carex–Equisetum* III where relative air humidity (RH) was significantly higher in opaque chambers with fan (DF) than in transparent with fan (TF) (Table S1 in the Supplement).

A pronounced diurnal methane emission dynamic was observed for BA *Phragmites–Carex* and GK *Phragmites–Lemna*, much stronger than for any other site (Fig. 2). Significantly different methane emissions between opaque and transparent chambers, however, were only found for GK *Typha–Hydrocharis* and GK *Carex–Lysimachia* (Table S1 in the Supplement). Measurements with TF chambers resulted here in 1.2 and 1.1 times higher emission estimates as compared to DF. Also for BA *Eriophorum–Carex* I measurements with TF gave higher results than DF (factor 1.09), but the difference was not significant (Fig. 2). For all other sites the ratio of TF/DF was equal one. Methane emissions measured by opaque chambers without head space mixing (D) were slightly but not significantly below that of DF chambers (Table S1 in the Supplement).

The findings of the chamber intercomparison were used to correct the measured growing season fluxes from GK *Typha–Hydrocharis* and GK *Carex–Lysimachia* which were multiplied by the TF/DF ratio of 1.2 to account for potential reduction of convective gas transport in *Typha latifolia* by shading with the regularly applied opaque chambers without fan. The factor 1.2 was applied for GK *Carex–Lysimachia* instead of 1.1, because *Typha latifolia* was present in all plots of that site, with the exception of plot I in 2012, where the diurnal chamber intercomparison took place (Table 2). Fluxes from the other sites were not corrected because chamber effects were not significant.

3.3.2 Annual methane emissions

The Lloyd–Taylor models generally reflected the temperature control of methane fluxes, were robust towards single events of extremely high or low fluxes, and allowed for comprehensive error calculation. Model performance was better in the first (median NSE = 0.55, range from 0.05 to 0.85) than in the second year (median NSE = 0.42, −0.25 to 0.76). Best first year models (NSE = 0.77 to 0.85) were that of GK *Carex–Lysimachia* I, *Phragmites–Lemna* I, and of all plots of BA *Carex–Equisetum*. Best models of the second year (NSE = 0.58 to 0.76) were of BA *Carex–Equisetum* III, GK *Carex–Lysimachia* II, and of all plots of BA *Eriophorum–Carex*. Low NSE values were found for most models of BA *Phragmites–Carex* and GK *Phragmites–Lemna*. Negative NSEs indicated poor performance of the second year methane models of BA *Phragmites–Carex* I and III, and GK *Phragmites–Lemna* III. The second year model of GK *Phragmites–Lemna* III and BA *Phragmites–Carex* III did not explain the very high emissions in August 2011 (Figs. 3h and 4h). Both, and the second year model of BA *Phragmites–Lemna* I, overestimated emissions in spring and early summer 2012. Annual emissions calculated alternatively for the mentioned plots and second year by linear interpolation were 25, 28, and 118 $\mathrm{g\,CH_4-C\,m^{-2}\,yr^{-1}}$, compared to 30, 32, and 139 $\mathrm{g\,CH_4-C\,m^{-2}\,yr^{-1}}$ derived by the temperature driven Lloyd–Taylor methane model, and lie within the 90 % confidence intervals of the latter (Table S2 in the Supplement). The Lloyd–Taylor models were therefore accepted for the described plots despite of negative NSE.

Annual methane emissions at Barcianicha from BA *Phragmites–Carex* were for the first and second year 42 and 36 $\mathrm{g\,CH_4-C\,m^{-2}\,yr^{-1}}$ (Table 3). Emissions were lower from BA *Carex-Equisetum* (17 and 13 $\mathrm{g\,CH_4-C\,m^{-2}\,yr^{-1}}$) and BA *Eriophorum–Carex* (10 and 11 $\mathrm{g\,CH_4-C\,m^{-2}\,yr^{-1}}$). Wide confidence intervals on the plot level and considerable small scale variability of methane emissions from BA *Phragmites–Carex* resulted in large uncertainties on the site level (Fig. 5, Table 3). Small scale spatial methane emission variability of BA *Phragmites–Carex* was 6.4 ± 2.7 $\mathrm{g\,CH_4-C\,m^{-2}\,yr^{-1}}$ (Table 4). For BA *Carex–Equisetum* it was 1.4 ± 0.7 $\mathrm{g\,CH_4-C\,m^{-2}\,yr^{-1}}$ and for BA *Eriophorum–Carex* only 0.5 ± 0.2 $\mathrm{g\,CH_4-C\,m^{-2}\,yr^{-1}}$. Inter-annual variability of methane emissions from BA *Phragmites–Carex* was 3.0±3.6 $\mathrm{g\,CH_4-C\,m^{-2}\,yr^{-1}}$, from BA *Carex–Equisetum* 2.3±0.5 $\mathrm{g\,CH_4-C\,m^{-2}\,yr^{-1}}$, and from BA *Eriophorum–Carex* 0.5±0.0 $\mathrm{g\,CH_4-C\,m^{-2}\,yr^{-1}}$ (Table 4). Maximum methane emissions at Barcianicha occurred from June to August at BA *Eriophorum–Carex* and BA *Carex–Equisetum* but at BA *Phragmites–Carex* only in July and August (Fig. 3). Local emission peaks were measured at BA *Phragmites–Carex* end of April–begin of May.

Methane emissions from Giel’čykaŭ Kašyl’ were higher than from Barcianicha. GK *Phragmites–Lemna* had in both years the highest methane emissions of all sites (100 and 101 $\mathrm{g\,CH_4-C\,m^{-2}\,yr^{-1}}$ in the first and second year, respectively). Emissions from GK *Carex–Lysimachia* were 86 and 85 $\mathrm{g\,CH_4-C\,m^{-2}\,yr^{-1}}$, and from GK *Typha–Hydrocharis* 60 and 68 $\mathrm{g\,CH_4-C\,m^{-2}\,yr^{-1}}$ (Table 3). Largest methane emissions from all Giel’čykaŭ Kašyl’ sites occurred during the summer months (Fig. 4). Summer emissions from GK *Phragmites*–*Lemna* were much higher in 2011 as compared to 2010 and 2012. Methane emission from Giel’čykaŭ Kašyl’ sites considerably varied among plots and between years (Fig. 5, Table 4). Inter-annual variability of methane emissions was $11.6 \pm 2.8\,\mathrm{g\,CH_4-C\,m^{-2}\,yr^{-1}}$ for GK *Phragmites*–*Lemna*, $4.2 \pm 2.9\,\mathrm{g\,CH_4-C\,m^{-2}\,yr^{-1}}$ for GK *Typha*–*Hydrocharis*, and $1.2 \pm 0.9\,\mathrm{g\,CH_4-C\,m^{-2}\,yr^{-1}}$ for GK *Carex*–*Lysimachia*. Small scale variability was higher for GK *Phragmites*–*Lemna* and GK *Carex*–*Lysimachia* (24.2 ± 10.0 and $10.9 \pm 8.3\,\mathrm{g\,CH_4-C\,m^{-2}\,yr^{-1}}$, respectively), but for GK *Typha*–*Hydrocharis* similar to inter-annual variability ($3.2 \pm 3.2\,\mathrm{g\,CH_4-C\,m^{-2}\,yr^{-1}}$). Large spatial variability is also reflected by the confidence intervals on the site level, which are wider for GK *Carex*–*Lysimachia* and GK *Phragmites*–*Lemna* as compared to GK *Typha*–*Hydrocharis* (Table 3).

3.4 Nitrous oxide emissions

Emissions of N_2O from all plots were around zero (Fig. 5e and f). Maximum plot emissions were around $0.5\,\mathrm{g\,N_2O-N\,m^{-2}\,yr^{-1}}$, but were usually compensated for by similar large uptakes in a neighbour plot or the other year. The overlap of the 90 % confidence of all sites, plots and years indicates that N_2O emissions were not significantly different among them.

3.5 Correlations between annual GHG emissions and site parameters

Peat characteristics were similar among all plots (Table 1) and there was only a weak correlation between annual methane emissions and C/N ratio, as well as between annual net CO_2 exchange and pH (Spearman’s $\rho = -0.50^*$ and $0.40'$, respectively, $'\ P \leq 0.05$; $^*\ P \leq 0.01$, $n = 36$; i.e. peat characteristics of 18 plots were correlated with annual fluxes of these plots of two GHG measuring years).

Median annual water level was not correlated with R_{eco}, very strongly with GPP, and weaker with NEE and CH_4 emissions (Fig. 6). Correlations of water levels with

R_{eco}, GPP, NEE and CH_4, were highly significant when GK *Typha–Hydrocharis* and GK *Carex–Lysimachia* were excluded from the analysis (Fig. 6, ρ in brackets). Correlations of water level with NEE and CH_4 and were also strong for Barcianicha alone ($\rho = -0.60^{**}$, 0.85^{***}, respectively, ** $P \leq 0.001$; *** $P \leq 0.0001$, $n = 18$).

Total above ground biomass carbon harvested after the second measuring year strongly correlated with the second year annual balances of CH_4, R_{eco} and GPP, but not with NEE (Fig. 6). Without GK *Typha–Hydrocharis* and GK *Carex–Lysimachia* correlations between biomass and balances of R_{eco} and GPP were stronger and the correlation between biomass and NEE became highly significant. When only Barcianicha was analysed, correlation between biomass and methane emissions where not significant, but correlations between biomass and R_{eco}, GPP, and NEE were strong ($\rho = 0.98^{***}$, -0.98^{***}, -0.95^{**}, respectively, $n = 9$).

Annual CH_4 emissions did not correlate with annual NEE, but strongly with R_{eco} and GPP (Fig. 6). Excluding GK *Typha–Hydrocharis* and GK *Carex–Lysimachia* resulted in highly significant correlation between methane and NEE (Fig. 6, $\rho = -0.83$, $P < 0.0001$, $n = 30$). For Barcianicha alone correlation between NEE and CH_4 emissions was also significant ($\rho = -0.67$, $P = 0.0028$, $n = 18$).

As expected, within-site variation of R_{eco} and absolute GPP generally scaled with biomass. (Fig. 6). Methane emissions increased among plots of BA *Phragmites–Carex* with increasing absolute GPP and R_{eco} and all three fluxes were positively related to above ground biomass. A positive relation between biomass and methane occurred on the small scale also for GK *Carex–Lysimachia*, while at GK *Phragmites–Lemna* methane emissions tended to decrease with increasing net CO_2 uptake (Fig. 6).

3.6 Carbon and GHG-balances of sites

GK *Phragmites–Lemna* and BA *Phragmites–Carex* were strong, and BA *Eriophorum–Carex* and BA *Carex–Equisetum* weak carbon sinks, while GK *Typha–Hydrocharis* and GK *Carex–Lysimachia* released high amounts of carbon (Table 3).

Net uptake of carbon dioxide and emissions of methane by Barcianicha sites nearly compensated each other with respect to their global warming potential for a time horizon of 100 years (Myhre et al., 2013; Table 5). In both years the Barcianicha sites were very small GHG sources and in the first year BA *Phragmites–Carex* a small GHG sink, but the uncertainties of the GHG balances of the latter site were large. Compensation for the warming effect of high methane emissions was achieved at Giel’čykaŭ Kašyl’ only in the second year by GK *Phragmites–Lemna* thanks to extremely high NEE. The site was a moderate GHG source in the first year when methane emissions were similar to the second year but NEE two times smaller. GK *Typha–Hydrocharis* and GK *Carex–Lysimachia* were strong methane sources, too. At the same time they were mostly small CO_2 sources, and as a result, significant GHG emitters. However, confidence intervals of GHG emissions from the Giel’čykaŭ Kašyl’ sites were very large. The role of N_2O exchange was negligible for the GHG-balances of all sites.

4 Discussion

4.1 Robustness of annual GHG balances

4.1.1 Methane

The pronounced diurnal methane emission dynamics from BA *Phragmites–Carex* and GK *Phragmites–Lemna* with fivefold flux increases from morning to midday result from active air transport in *Phragmites australis* aerenchyma in the growing season related to sun light (Armstrong and Armstrong, 1991; Brix et al., 1992; Armstrong et al., 1996). In contrast to other studies (Van der Nat and Middelburg, 2000; Günther et al., 2013) we did not find a significant impact of chamber transparency on measured methane emission rates, maybe because enclosed plants were connected by rhizomes with culms outside the chamber. Such connection is supposed to allow for pressure propagation and continuation of unrestrained convective gas flow (Juutinen et al., 2004; Minke et al., 2014). Consequently the application of opaque chambers has not biased annual emission estimates from the *Phragmites australis* sites. But frequency of measurements and the selected annual model based on daily soil temperature as driver did not account for diurnal flux variability. Day-to-day variability and seasonal variation of average daily emissions from *Phragmites australis* stands are strongly controlled by sediment temperature (Kim et al., 1998; Kankaala et al., 2004), which supports our decision to use soil temperature for modelling methane emission. However, a single measurement at any time during daylight does not represent the daily emission average and would for the monitored days (Fig. 2) mostly have resulted in equal or higher estimates as compared to the 24 hour mean (daily average calculated from transparent chamber measurements were 6.75 $\mathrm{mg\,CH_4-C\,m^{-2}\,h^{-1}}$ from BA *Phragmites–Carex* II, and 9.54 $\mathrm{mg\,CH_4-C\,m^{-2}\,h^{-1}}$ from GK *Phragmites–Lemna* II). So, possibly the high emission events in summer 2011 not explained by the models of BA *Phragmites–Carex* III and GK *Phragmites–Lemna* III were daily maxima and the models were still at or just below the daily averages. Fluxes in spring and early summer 2012 were most likely overestimated by the models of BA *Phragmites–Carex* I and III, because they were measured predominantly at midday and early afternoon of clear or only partly clouded days and can therefore be expected to exceed the daily average. The same holds for summer fluxes in 2012 at GK *Phragmites–Lemna* III. In summary, our approach tended to overestimate the real emissions at the *Phragmites australis* sites.

The less pronounced diurnal methane emission dynamics of GK *Typha–Hydrocharis* with only a short term peak in the mid-morning (first day) and the reduction of emissions when chambers were shaded agree with other studies of *Typha latifolia* (Chanton et al., 1993; Whiting and Chanton, 1996). Similar to *Phragmites australis*, green parts of *Typha latifolia* pressurize during daylight which drives convective gas transport and accelerates methane efflux (Brix et al., 1992; Whiting and Chanton, 1996). Although no transient emission peak was observed at the second day, the ratio of transparent/opaque chamber was the same for both days (Table S1). Other researchers calculated similar transparent/opaque ratios for *Typha latifolia* (1.1 – Whiting and Chanton, 1996; 1.3 – Günther et al., 2013). However, we do not know the variability of the ratio under different weather conditions. Therefore we used the correction factor 1.2 for total daily methane emissions during the growing season, despite the irrelevance of chamber transparency at night time. Calculated annual emissions will consequently be at the high end of real emissions from the site.

Typha latifolia did not grow on the diurnal monitored plot I of GK *Carex–Lysimachia* in summer 2012. Instead *Carex elata* dominated. Gas transport in sedges is driven only by diffusion (Armstrong, 1979; King et al., 1998). Existing studies led to different outcomes regarding the effect of shading by chambers. Shading reduced methane emissions from *Carex aquatilis* (Morrissey et al., 1993) and *Carex allivescers* (Hirota et al., 2004), but not from *Carex limosa* and *C. rostrata* (Whiting and Chanton, 1992) and *C. acutiformis* (Günther et al., 2013). We do not know the reason for the small but significant shading impact on methane fluxes from plot I of GK *Carex–Lysimachia*. However, *Typha latifolia* was, except for this plot in summer 2012, always present at all plots of GK *Carex–Lysimachia* (Table 2). Correction of daily fluxes from GK *Carex–Lysimachia* using the factor 1.2 from GK *Typha–Hydrocharis* accounted for this. Again, the calculated annual CH_4 emissions will represent the high end of real emissions from the site.

The lack of any shading impact on methane emissions from BA *Eriophorum–Carex* and BA *Carex–Equisetum* corresponds to the findings of Joabsson et al. (1999) and Whiting and Chanton (1992) for *Eriophorum angustifolium* and *Carex rostrata*.

4.1.2 Carbon dioxide

The two approaches used to model CO_2 exchange rates resulted in very similar annual balances. Plot-wise annual R_{eco} calculated with APPROACH ONE was on average 5 % (±5 %, $n = 36$) below APPROACH TWO, while the GPP sink was higher by 1 % (±3 %, $n = 36$). Resulting annual net CO_2 uptake was consequently on average stronger for APPROACH ONE than for APPROACH TWO. The mean difference of NEE between both approaches was $43 \pm 41\,\mathrm{g\,CO_2{-}C\,m^{-2}\,yr^{-1}}$ ($n = 36$), but $77 \pm 40\,\mathrm{g\,CO_2{-}C\,m^{-2}\,yr^{-1}}$, when calculated only for *Phragmites australis* plots ($n = 12$). This indicates that measured fluxes and general modelling assumptions, i.e. the temperature relation of R_{eco} and PAR relation of GPP were robust towards differences in flux calculation and model parameterization. Also the good results of the cross validations of the models of APPROACH ONE at all sites indicate a high reliability of the results.

The net annual CO_2 sink of the *Phragmites australis* sites was large, especially at GK *Phragmites–Lemna*. The first year NEE of this site equalled the estimate of Brix et al. (2001; Table 7) but the second year uptake was two times higher. To test for plausibility we roughly estimated the carbon flux partitioning in the ecosystem from independent data. We estimated the net primary production (NPP) based on measured green above ground biomass and published ratios between above ground and below ground biomass production (Table 6). Using NPP, NEE, and GPP we calculated heterotrophic and autotrophic respiration (Rh and Ra, Table 6) and evaluated their meaningfulness. As expected because of inundation, heterotrophic respiration was low, ranging between 77 and 114 $\mathrm{g\,CO_2-C\,m^{-2}\,yr^{-1}}$. The ratio of heterotrophic respiration to methane emissions (CO_2-C / CH_4-C) was for BA *Phragmites–Carex* 2.2 and 2.3 and for GK *Phragmites–Lemna* 1.0 and 1.1, what is similar to ratios found in incubation experiments for the upper peat layer (1.6) and organic bottom sediments (0.7) of a flooded former fen grassland (Hahn-Schöfl et al., 2011). Calculated autotrophic respiration was half of GPP, but differed considerably between years (43 to 61 %). This may result to a large extent from the uncertainty of the estimates (especially of NPP), as the efficiency of converting GPP to NPP is generally assumed to be relatively constant (cf. Chapin et al., 2002). In summary, our very rough estimation resulted for the *Phragmites australis* sites in reasonable annual rates of heterotrophic respiration and shares between NPP and R_a.

4.2 Annual CO_2 and methane balances of similar sites

Annual methane emissions from BA *Eriophorum–Carex* and BA *Carex–Equisetum* were higher and NEE was lower as compared to a shallowly inundated cutover Atlantic blanket bog colonized by *Eriophorum angustifolium* ($CH_4 = 5.3\,g\,CH_4-C\,m^{-2}\,yr^{-2}$, NEE = $-348\,g\,CO_2-C\,m^{-2}\,yr^{-2}$; Table 7; Wilson et al., 2013). This could be due to climate differences, or caused by different soil properties, as the Atlantic bog peat was oligotrophic and very acid. Methane emissions from a *Eriophorum angustifolium–Carex rostrata* site in another rewetted cutover Irish bog were lower and dropped from $3.2\,g\,CH_4-C\,m^{-2}\,yr^{-2}$, in a wet year (WL ~ 5 cm above surface) to $2.4\,g\,CH_4-C\,m^{-2}\,yr^{-2}$ in a drier year (WL ~ 6 cm below surface) (Wilson et al., 2009). This site, however, was a CO_2 source (163 and $408\,g\,CO_2-C\,m^{-2}\,yr^{-2}$ in the wet and drier year, respectively, Wilson et al., 2007) probably due to additional CO_2 production when water from the calcareous subsoil came into contact with the slightly acidic residual peat (cf. Harpenslager et al., 2015).

Methane emissions from BA *Phragmites–Carex* compared well to the shallow water inner reed zone ($33\,g\,CH_4-C\,m^{-2}\,yr^{-1}$) and that from GK *Phragmites-Lemna* to the deep water outer reed zone ($122\,g\,CH_4-C\,m^{-2}\,yr^{-1}$) of lake Lake Vesijärvi in Southern Finland (Table 7; Kankaala et al., 2004). Methane emissions from a *Phragmites australis* dominated, shallowly inundated marsh in north-central Nebraska, USA (Kim et al., 1998) as well as from wet *Phragmites australis* stands in a rewetted Dutch fen (Hendriks et al., 2007) were with 60, respectively $88\,g\,CH_4-C\,m^{-2}\,yr^{-1}$ between both *Phragmites australis* sites of the present study. Annual NEE fluxes were more than ten times higher than at a freshwater tidal reed wetland in NE China, though above ground biomass was comparable (Zhou et al., 2009). The differences result from smaller ratios of R_{eco} to GPP in the present (0.58 ± 0.09, $n = 4$) compared to the tidal reed study (0.95) and can be explained by permanent inundation of BA *Phragmites–Carex* and GK *Phragmites–Lemna*, and consequently low heterotrophic respiration (see Sect. 4.1.2), while the soil of the tidal reed wetland was periodically aerated. The importance of water level was also evident for a *Phragmites australis* site in a rewetted former grassland fen in NE Germany that sequestrated $83\,g\,CO_2-C\,m^{-2}\,yr^{-2}$ and emitted $11\,g\,CH_4-C\,m^{-2}\,yr^{-1}$ in a exceptionally wet year (WL at surface) but released

$68\,g\,CO_2-C\,m^{-2}\,yr^{-2}$ and only $1\,g\,CH_4-C\,m^{-2}\,yr^{-1}$ in a typical year (WL below surface; Günther et al., 2014).

Annual methane and CO_2 fluxes from floating tall sedge – cattail mats are not reported in the literature. Methane emissions from GK *Typha–Hydrocharis* and GK *Carex–Lysimachia* were higher compared to a pristine water saturated sedge fen (dominated by *Carex aquatilis*) in the southern Rocky Mountains (30 to $34\,g\,CH_4-C\,m^{-2}\,yr^{-2}$; Table 7; Wickland et al., 2001) or to *Carex acutiformis and Typha latifolia* sites during the wet year in the above mentioned rewetted fen grassland (47 and $10\,g\,CH_4-C\,m^{-2}\,yr^{-2}$, respectively; Günther et al., 2014). They were comparable to temperate *Typha latifolia* ($82\,g\,CH_4-C\,m^{-2}\,yr^{-2}$; Whiting and Chanton, 2001) and *T. angustifolia* marshes ($51\,g\,CH_4-C\,m^{-2}\,yr^{-2}$,Chu et al., 2015; $127\,g\,CH_4-C\,m^{-2}\,yr^{-2}$, Strachan et al., 2015). The constantly high water levels made us expect a net CO_2 uptake at GK *Typha–Hydrocharis* and GK *Carex–Lysimachia*, as was found for *Typha latifolia* and *T. angustifolia* marshes (Whiting and Chanton, 2001; Strachan et al., 2015), for a water saturated temperate sedge fen in the Czech Republic (Dušek et al., 2012), and in the wet year for *Carex acutiformis and Typha latifolia* (Günther et al., 2014). Both sites, however, were CO_2 and carbon sources. Net CO_2 emissions, though smaller as compared to our study, were also observed from a wet sedge fen in the southern Rocky Mountains (77 to $84\,g\,CO_2-C\,m^{-2}\,yr^{-1}$; Wickland et al., 2001), and in two of three years from a water saturated *Typha angustifolia* marsh (Chu et al., 2015). Chu et al. (2015) explain their findings by abnormal climatic conditions. However, climatic conditions during the first year of the present study were similar to the long term average and other factors, like reduced GPP because of shading from old standing leafs (Rocha et al., 2008) may have been important, as there was much dry biomass present. Also the high water levels and their strong fluctuations may have imposed stress on the vegetation (Dušek et al., 2012), as indicated by changes in the cover of the dominant species between years (Table 2) and the early aging of the sedges. High R_{eco} fluxes from both sites could be the result of high maintenance respiration because of environmental stress (Chapin et al., 2002) combined with increased heterotrophic respiration from decomposing dead plant material which formed the main part of the sedge tussocks (estimated from photographic documentation). This indicates that the plant communities were not well adapted to the present conditions and may represent a transient development stage.

4.3 Controls of annual GHG emissions

The average GHG emissions from all studied sites were with 12.2 t CO_2 eq ha^{-1} yr^{-1} similar to GHG emissions from rewetted rich temperate fens (10 t CO_2 eq ha^{-1} yr^{-1}) as given by Blain et al. (2014). However, GHG emissions and carbon balances differed considerably among the studied sites. BA *Eriophorum–Carex*, BA *Carex–Equisetum*, BA *Phragmites–Carex* and GK *Phragmites–Lemna* had on average low GHG emissions (2.3, 4.2, –1.7, and 4.2 t CO_2 eq ha^{-1} yr^{-1}, respectively), and were weak to strong carbon sinks (–36, –17, –390, and –795 g C m^{-2} yr^{-1}), confirming that important aims of peatland rewetting, i.e. restoration of the carbon sink function and reduction of GHG emissions have been largely achieved. Net carbon losses from GK *Typha–Hydrocharis* and GK *Carex–Lysimachia* of the terrestrialization zone (83 and 276 g C m^{-2} yr^{-1}, respectively), in contrast, were similar as from peat extraction sites (280 g C m^{-2} yr^{-1} – Drösler et al., 2014) and GHG emissions (25.1 and 39.1 t CO_2 eq ha^{-1} yr^{-1}) were even comparable to deep-drained temperate fen grassland (26 t CO_2 eq ha^{-1} yr^{-1} – Drösler et al., 2014; 65 t CO_2 eq ha^{-1} yr^{-1} – Eickenscheidt et al., 2015). To understand reasons for these differences among sites we now look on potential drivers for individual GHG fluxes.

4.3.1 Water table

Significant correlation between annual water level and methane emissions, as well as between water level and CO_2 fluxes (Fig. 6) indicate that emission differences among sites may be caused by water level differences. In drained peatlands water table depth defines the thickness of the aerobic zone and consequently the rate of peat oxidation

(Couwenberg et al., 2011). As discussed above (4.2) all sites of the present study were permanently water saturated and heterotrophic respiration was consequently low. Water levels link to CO_2 flux differences among sites more indirectly, by influencing other variables that control CO_2 fluxes, for example vegetation composition.

Methane emissions are affected by water table position as it defines the thickness of the oxidation zone at the soil surface or – under flooded conditions – in the water column (Couwenberg and Fritz, 2012). However, when aerenchymous plants are abundant, as in the present study, they dominate the gas exchange and methane bypasses the oxygenated water column (Whiting and Chanton, 1992; Chanton and Whiting, 1995; Couwenberg and Fritz, 2012). So, water level influenced methane emissions of the studied sites also mainly by influencing plant species distribution.

Nitrous oxide emissions were for all sites about zero, what is the result of permanent water saturatation and agrees with other studies from rewetted fens (Hendriks et al., 2007; Couwenberg et al., 2011; Wilson et al., 2013).

4.3.2 Nutrient conditions

Nutrient conditions as indicated by vegetation composition were dominantly controlled by water supply (river and grassland drainage water for Giel’čykaŭ Kašyl’, groundwater for Barcianicha), while surface peat (eutrophic at both sites) was less important. CO_2 fluxes and methane emissions were higher from the eutrophic Giel’čykaŭ Kašyl’ as compared to the mesotrophic Barcianicha. As for water level, nutrient conditions affected GHG emissions via their influence on vegetation. Eutrophic conditions supported the establishment of more productive plant species at Giel’čykaŭ Kašyl’ compared to the mesotrophic Barcianicha. Also the productivity of *Phragmites australis* differed strongly between both peatlands. This is in line with Blain et al. (2014) who found that methane and CO_2 emissions are higher from rich temperate rewetted fens as compared to poor fens and bogs. Our results indicate that rich temperate rewetted fens may be further subdivided into mesotrophic and eutrophic to account for significantly different methane emissions.

4.3.3 Vegetation and plant productivity

In both peatlands the *Phragmites australis* communities grew at higher water tables and were larger CO_2 sinks and CH_4 sources as compared to the sedge communities in the shallower areas. Plant productivity was the main control of CO_2 fluxes, as indicated by the strong correlation between biomass and NEE for all sites except GK *Typha–Hydrocharis* and GK *Carex–Lysimachia* (Fig. 6). Small scale variability, calculated as absolute difference between annual plot emissions and annual site emissions was larger for NEE ($92 \pm 108\,\mathrm{g\,CO_2-C\,m^{-2}\,yr^{-1}}$) than for methane emissions ($8 \pm 10\,\mathrm{g\,CH_4-C\,m^{-2}\,yr^{-1}}$). Also inter-annual variability, calculated plot-wise as the absolute difference of annual emissions from the two years mean, was larger for NEE ($116 \pm 119\,\mathrm{g\,CO_2-C\,m^{-2}\,yr^{-1}}$) as compared to methane emissions ($4 \pm 4\,\mathrm{g\,CH_4-C\,m^{-2}\,yr^{-1}}$). Both can be explained by the fact that CO_2-fluxes are more directly linked to plant productivity than methane fluxes (Hyvönen et al., 1998; Bonneville et al., 2008; Schneider et al., 2012). However, also interannual and small scale variability of methane emissions increased with above ground biomass and GPP (Fig. 6), and was larger in Giel'čykaŭ Kašyl' compared to Barcianicha, and in both peatlands for the *Phragmites australis* sites. This is most likely due to control of vegetation and plant productivity on methane emissions, as indicated by the highly significant correlation between methane emissions and net CO_2 uptake (Fig. 6, when analysed without the terrestrialization zone) and between methane emissions and biomass, and can be explained by supply of organic material and by plant mediated gas exchange (Whiting and Chanton, 1993; Chanton et al., 1995; Bellisario et al., 1999; Whalen, 2005). Fresh organic substrates were rather limited at Barcianicha, where the thin layer of litter and many bare peat patches indicated the lack of plant litter substrate for methane generation. More emissions can be expected when more litter accumulates (Waddington and Day, 2007). Plant litter was more abundant at Giel'čykaŭ Kašyl', certainly because of higher plant productivity, but also because of longer period since rewetting. This may explain the strong correlation between NEE and methane emissions at Barcianicha, but not at Giel'čykaŭ Kašyl'. Methane production was obviously less depending on actual primary production, especially in the terrestrialization zone of Giel'čykaŭ Kašyl'. Methane emissions from GK *Typha–Hydrocharis* and GK *Carex–Lysimachia* were high and at least partly fuelled by old litter, because both sites were no net CO_2 sinks. Also allochthonous carbon can not be excluded as a substrate for methane production at Giel'čykaŭ Kašyl' (Chu et al., 2015), for example from floating plants like *Lemna trisulca* that form detritus with a much higher methane production potential compared to *Phragmites australis* litter (Kankaala et al., 2003).

5 Conclusions

The eutrophic peatland Giel'čykaŭ Kašyl' with deep standing water had a large carbon sink potential, but also a high risk of local net CO_2 losses. The site varied spatially and temporally between being a small net GHG sink and a large source because of high methane emissions. The mesotrophic peatland Barcianicha with shallow, constant water levels, in contrast, constituted a smaller but more stable carbon sink and only a small GHG source. Both net CO_2 uptake and methane emissions were strongly linked to vegetation and plant productivity, which in turn were related to water level and nutrient conditions. Emission variability increased with productivity of sites. This implies that the formulation of robust emission factors requires more long-term and spatially resolved GHG emission studies in case of high-productive than for low-productive vegetation types and mire ecosystems.

Unexpectedly high carbon losses and GHG emissions from the terrestrialization zone of Giel'čykaŭ Kašyl' were most likely caused by vegetation suffering from high and strongly fluctuating water levels. The exact sources of these high emissions, as well as the duration and successional pathway of the supposed transitional phase require further study.

Our study indicates that permanent, shallow inundation of cutover temperate fens is a more suitable measure to arrive at low GHG emissions than deep flooding, as the latter may create unfavourable conditions for plant growth and carbon sequestration, and the site may remain a strong net GHG source because of high methane emissions. If shallow flooding cannot be practically realized, deep flooding seems to be a reasonable alternative, at least when *Phragmites australis* can be established. The risk of high GHG emissions is higher for eutrophic as compared to mesotrophic peatlands. In spite of the possible high emissions, flooding still has to be preferred over keeping temperate fen grasslands deeply drained, because the GHG emissions from the latter are similar to those from the hotspot of our study, the eutrophic terrestrialization zone, but exceed those from the spatially dominant flooded *Phragmites australis* reed by far.

The Supplement related to this article is available online at doi:10.5194/bgd-12-17393-2015-supplement.

Acknowledgements. This study was funded by the KfW Entwicklungsbank in the framework of the International Climate Initiative of the German Federal Ministry for the Environment, Nature Conservation and Nuclear Safety (BMU) under BMU project Reference No.: II. C. 53, and by the Centre for International Migration and Development (CIM) and the Royal Society for the Protection of Birds (RSPB). We thank APB – BirdLife Belarus and the National Academy of Sciences of Belarus for creating ideal research conditions, Hans Joosten for support in designing the study and for commenting the manuscript, Nadzeya Liashchynskaya, Hanna Grabenberger, Aleksandr Novik, Nikolaj Belovezhkin, Konstantin Timokhov and Aleksandr Pavlyuchenko for help in the field, Sergej Zui for construction and maintenance of measuring equipment, Vyacheslav Rakovich, Petr Boldovskij and Vadim Protasevich for information on land use history, Michel Bechthold for advice on evaluation of the hydrological data, Roland Fuß, Katharina Leiber-Sauheitl and Thomas Leppelt for consultations on statistical issues.

References

Abramov, I. I. and Volkova, L. A.: Handbook of Mosses of Karelia, KMK Scientific Press Delphos, Moscow, 1998.

AG Boden: Bodenkundliche Kartieranleitung (Soil survey manual), 5th Edn., Hannover, 2005.

Alm, J., Talanov, A., Saarnio, S., Silvola, J., Ikkonen, E., Aaltonen, H., Nykänen, H., and Martikainen, P. J.: Reconstruction of the carbon balance for microsites in a boreal oligotrophic pine fen, Finland, Oecologia, 110, 423–431, 1997.

Armstrong, J. and Armstrong, W.: A convective through–flow of gases in *Phragmites australis* (Cav.) Trin. Ex Steud., Aquat. Bot., 39, 75–88, 1991.

Armstrong, J., Armstrong, W., Beckett, P. M., Halder, J. E., Lythe, S., Holt, R., and Sinclair, A.: Pathways of aeration and the mechanisms and beneficial effects of humidity and Venturi-induced convections in *Phragmites australis* (Cav.) Trin. Ex Steud., Aquat. Bot., 54, 177–198, 1996.

Armstrong, W.: Aeration in higher plants, Adv. Bot. Res., 7, 236–332, 1979.

Asaeda, T., Manatunge, J., Roberts, J., and Hai, D. N.: Seasonal dynamics of resource translocation between the aboveground organs and age-specific rhizome segments of *Phragmites australis*, Environ. Exp. Bot., 57, 9–18, 2006.

Bellisario, L. M., Bubier, J. L., Moore, T. R., and Chanton, J. P.: Controls on CH_4 emissions from a northern peatland, Global Biogeochem. Cy., 13, 81–91, 1999.

Beyer, C. and Höper, H.: Greenhouse gas exchange of rewetted bog peat extraction sites and a *Sphagnum* cultivation site in northwest Germany, Biogeosciences, 12, 2101–2117, doi:10.5194/bg-12-2101-2015, 2015.

Blain, D., Murdiyarso, D., Couwenberg, J., Nagata, O., Renou-Wilson, F., Sirin, A., Strack, M., Tuittila, E.-S., Wilson, D., Evans, C. D., Fukuda, M., and Parish, F.: Chapter 3: Rewetted organic soils, in: 2013 Supplement to the 2006 IPCC Guidelines for National Greenhouse Gas Inventories: Wetlands, edited by: Hiraishi, T., Krug, T., Tanabe, K., Srivastava, N., Baasansuren, J., Fukuda, M., and Troxler, T. G., IPCC, Switzerland, 3.1–3.42, 2014.

Bonneville, M. C., Strachan, I. B., Humphreys, E. R., and Roulet, N. T.: Net ecosystem CO_2 exchange in a temperate cattail marsh in relation to biophysical properties, Agr. Forest Meteorol., 148, 69–81, 2008.

Brix, H., Sorrell, B. K., and Orr, P. T.: Internal pressurization and convective gas flow in some emergent freshwater macrophytes, Limnol. Oceanogr., 37, 1420–1433, 1992.

Brix, H., Sorrell, B. K., and Lorenzen, B.: Are *Phragmites*-dominated wetlands a net source or net sink of greenhouse gases?, Aquat. Bot., 69, 313–324, 2001.

Chanton, J. P. and Whiting, G. J.: Trace gas exchange in freshwater and coastal marine environments: ebullition and transport by plants, in: Biogenic Trace Gases: Measuring Emissions from Soil and Water, edited by: Matson, P. A. and Harriss, R. C., Blackwell Science Ltd., Oxford, UK, 98–125, 1995.

Chanton, J. P., Whiting, G., Happell, J., and Gerard, G.: Contrasting rates and diurnal patterns of methane emission from different types of vegetation, Aquat. Bot., 46, 111–128, 1993.

Chanton, J. P., Bauer, J. E., Glaser, P. A., Siegel, D. I., Kelley, C. A., Tyler, S. C., Romanowicz, E. H., and Lazrus, A.: Radiocarbon evidence for the substrates supporting methane formation within northern Minnesota peatlands, Geochim. Cosmochim. Ac., 59, 3663–3668, 1995.

Chapin III, F. S., Matson, P. A., and Mooney, H. A.: Principles of Terrestrial Ecosystem Ecology, Springer-Verlag, New York, 2002.

Chu, H., Gottgens, J. F., Chen, J., Sun, G., Desai, A. R., Ouyang, Z., Shao, C., and Czajkowski, K.: Climatic variability, hydrologic anomaly, and methane emission can turn productive freshwater marshes into net carbon sources, Glob. Change Biol., 21, 1165–1181, doi:10.1111/gcb.12760, 2015.

Conrad, R., Schütz, H., and Babbel, M.: Temperature limitation of hydrogen turnover and methanogenesis in anoxic paddy soil, FEMS Microbiol. Ecol., 45, 281–289, 1987.

Couwenberg, J. and Fritz, C.: Towards developing IPCC methane "emission factors" for peatlands (organic soils), MaP, 10, 1–17, 2012.

Couwenberg, J., Augustin, J., Michaelis, D., and Joosten, H.: Emission Reductions from Rewetting of Peatlands, Towards a Field Guide for the Assessment of Greenhouse Gas Emissions from Central European Peatlands, Duene/RSPB, Greifswald/Sandy, 2008.

Couwenberg, J., Thiele, A., Tanneberger, F., Augustin, J., Bärisch, S., Dubovik, D., Liashchynskaya, N., Michaelis, D., Minke, M., Skuratovich, A., and Joosten, H.: Assessing greenhouse gas emissions from peatlands using vegetation as a proxy, Hydrobiologia, 674, 67–89, doi:10.1007/s10750-011-0729-x, 2011.

Daulat, W. E. and Clymo, R. S.: Effects of temperature and watertable on the efflux of methane from peatland surface cores, Atmos. Environ., 32, 3207–3218, 1998.

Dise, N. B., Gorham, E., and Verry, E. S.: Environmental factors controlling methane emissions from peatlands in Northern Minnesota, J. Geophys. Res., 98, 10583–10594, 1993.

Drösler, M.: Trace Gas Exchange and Climatic Relevance of Bog Ecosystems, southern Germany, Ph.D. thesis, Technische Universität München, München, 2005.

Drösler, M., Freibauer, A., Christensen, T. R., and Friborg, T.: Observations and status of peatland greenhouse gas emissions in Europe, in: The Continental-Scale Greenhouse Gas Balance of Europe, edited by: Dolman, H., Valentini, R., and Freibauer, A., Ecol. Stud., 203, 243–261, 2008.

Drösler, M., Verchot, L. V., Freibauer, A., Pan, G., Evans, C. D., Bourbonniere, R. A., Alm, J. P., Page, S., Agus, F., Hergoualc'h, K., Couwenberg, J., Jauhiainen, J., Sabiham, S., Wang, C., Srivastava, N., Borgeau-Chavez, L., Hooijer, A., Minkkinen, K., French, N., Strand, T., Sirin, A., Mickler, R., Tansey, K., and Larkin, N.: Chapter 2: Drained inland organic soils, in: 2013 Supplement to the 2006 IPCC Guidelines for National Greenhouse Gas Inventories: Wetlands, edited by: Hiraishi, T., Krug, T., Tanabe, K., Srivastava, N., Baasansuren, J., Fukuda, M., and Troxler, T. G., IPCC, Switzerland, 2.1–2.76, 2014.

Dušek, J., Žížková, H., Stellner, S., Czerný, R., and Květ, J.: Fluctuating water table affects gross ecosystem production and gross radiation use efficiency in a sedge-grass marsh, Hydrobiologia, 692, 57–66, doi:10.1007/s10750-012-0998-z, 2012.

Eickenscheidt, T., Heinichen, J., and Drösler, M.: The greenhouse gas balance of a drained fen peatland is mainly controlled by land-use rather than soil organic carbon content, Biogeosciences, 12, 5161–5184, doi:10.5194/bg-12-5161-2015, 2015.

Falge, E., Baldocchi, D., Olson, R., Anthoni, P., Aubinet, M., Bernhofer, C., Burba, G., Ceulemans, R., Clement, R., Dolman, H., Granier, A., Gross, P., Grünwald, T., Hollinger, D., Jensen, N.-O., Katul, G., Keronen, P., Kowalski, A., Lai, C. T., Law, B. E., Meyers, T., Moncrieff, J., Moors, E., Munger, J. W., Pilegaard, K., Rannik, Ü., Rebmann, C., Suyker, A., Tenhunen, J., Tu, K., Verma, S., Vesala, T., Wilson, K., and Wofsy, S.: Gap filling strategies for defensible annual sums of net ecosystem exchange, Agr. Forest Meteorol., 107, 43–69, 2001.

Gilmanov, T. G., Soussana, J. F., Aires, L., Allard, V., Ammann, C., Balzarolo, M., Barcza, Z., Bernhofer, C., Campbell, C. L., Cernusca, A., Cescatti, A., Clifton-Brown, J., Dirks, B. O. M., Dore, S., Eugster, W., Fuhrer, J., Gimeno, C., Gruenwald, T., Haszpra, L., Hensen, A., Ibrom, A., Jacobs, A. F. G., Jones, M. B., Lanigan, G., Laurila, T., Lohila, A., Manca, G., Marcolla, B., Nagy, Z., Pilegaard, K., Pinter, K., Pio, C., Raschi, A., Rogiers, N., Sanz, M. J., Stefani, P., Sutton, M., Tuba, Z., Valentini, R., Williams, M. L., and Wohlfahrt, G.: Partitioning European grassland net ecosystem CO_2 exchange into gross primary productivity and ecosystem respiration using light response function analysis, Agric. Ecosyst. Environ., 121, 93–120, 2007.

Günther, A., Jurasinski, G., Huth, V., and Glatzel, S.: Opaque closed chambers underestimate methane fluxes of *Phragmites australis* (Cav.) Trin. ex Steud., Environ. Monit. Assess., 186, 2151–2158, doi:10.1007/s10661-013-3524-5, 2013.

Günther, A., Huth, V., Jurasinski, G., and Glatzel, S.: The effect of biomass harvesting on greenhouse gas emissions from a rewetted temperate fen, GCB Bioenergy, 7, 1092–1106, doi:10.1111/gcbb.12214, 2014.

Hahn-Schöfl, M., Zak, D., Minke, M., Gelbrecht, J., Augustin, J., and Freibauer, A.: Organic sediment formed during inundation of a degraded fen grassland emits large fluxes of CH_4 and CO_2, Biogeosciences, 8, 1539–1550, doi:10.5194/bg-8-1539-2011, 2011.

Harpenslager, S. F., van Dijk, G., Kosten, S., Roelofs, J. G. M., Smolders, A. J. P., and Lamers, L. P. M.: Simultaneous high C fixation and high C emissions in *Sphagnum* mires, Biogeosciences, 12, 4739–4749, doi:10.5194/bg-12-4739-2015, 2015.

Helfter, C., Campbell, C., Dinsmore, K. J., Drewer, J., Coyle, M., Anderson, M., Skiba, U., Nemitz, E., Billett, M. F., and Sutton, M. A.: Drivers of long-term variability in CO_2 net ecosystem exchange in a temperate peatland, Biogeosciences, 12, 1799–1811, doi:10.5194/bg-12-1799-2015, 2015.

Hendriks, D. M. D., van Huissteden, J., Dolman, A. J., and van der Molen, M. K.: The full greenhouse gas balance of an abandoned peat meadow, Biogeosciences, 4, 411–424, doi:10.5194/bg-4-411-2007, 2007.

Hirota, M., Tang, Y., Hu, Q., Hirata, S., Kato, T., Mo, W., Cao, G., and Mariko, S.: Methane emissions from different vegetation zones in a Qinghai-Tibetan Plateau wetland, Soil Biol. Biochem., 36, 737–748, 2004.

Hoffmann, M., Jurisch, N., Albiac, B. E., Hagemann, U., Drösler, M., Sommer, M., and Augustin, J.: Automated modeling of ecosystem CO_2 fluxes based on periodic closed chamber measurements: a standardized conceptual and practical approach, Agr. Forest Meteorol., 200, 30–45, 2015.

Hyvönen, T., Ojala, A., Kankaala, P., and Martikainen, P. J.: Methane release from stands of water horsetail (*Equisetum fluviatile*) in a boreal lake, Freshwater Biol., 40, 275–284, 1998.

Joabsson, A., Christensen, T. R., and Wallén, B.: Influence of vascular plant photosynthetic rate on CH_4 emission from peat monoliths from southern boreal Sweden, Polar Res., 18, 215–220, 1999.

Joosten, H. and Clarke, D.: Wise Use of Mires and Peatlands – Background and Principles Including a Framework for Decision-Making, Saarijärvi, International Mire Conservation Group and International Peat Society, 2002.

Joosten, H., Tapio-Biström, M.-L., and Tol, S.: Peatlands – Guidance for Climate Change Mitigation by Conservation, Rehabilitation and Sustainable Use, FAO and Wetlands International, Rome, 2012.

Jurasinski, G., Koebsch, F., and Hagemann, U.: Flux: Flux Rate Calculation from Dynamic Closed Chamber Measurements, R Package Version 0.2-1, Rostock, 2012.

Juutinen, S., Alm, J., Larmola, T., Saarnio, S., Martikainen, P. J., and Silvola, J.: Stand-specific diurnal dynamics of CH_4 fluxes in boreal lakes: patterns and controls, J. Geophys. Res., 109, D19313, doi:10.1029/2004JD004782, 2004.

Kadastrovyj spravochnik “Torfyanoj fond Belorusskoj SSR” (Cadastral reference “Peat fond of the BSSR”), Minsk, 1979.

Kankaala, P., Käki, T., and Ojala, A.: Quality of detritus impacts on spatial variation of methane emissions from littoral sediment of a boreal lake, Arch. Hydrobiol., 157, 47–66, 2003.

Kankaala, P., Ojala, A., and Käki, T.: Temporal and spatial variation in methane emissions from a flooded transgression shore of a boreal lake, Biogeochemistry, 68, 297–311, 2004.

Kettunen, A., Kaitala, V., Alm, J., Silvola, J., Nykänen, H., and Martikainen, P. J.: Predicting variations in methane emissions from boreal peatlands through regression models, Boreal Environ. Res., 5, 115–131, 2000.

Kim, J., Verma, S. B., and Billesbach, D. P.: Seasonal variation in methane emission from a temperate Phragmites-dominated marsh: effect of growth stage and plant mediated transport, Glob. Change Biol., 5, 433–440, 1998.

King, J. Y., Reeburgh, W. S., and Regli, S. K.: Methane emission and transport by arctic sedges in Alaska: results of a vegetation removal experiment, J. Geophys. Res., 103, 29083–29092, 1998.

Knox, S. H., Sturtevant, C., Matthes, J. H., Koteen, L., Verfaillie, J., and Baldocchi, D.: Agricultural peatland restoration: effects of land-use change on greenhouse gas (CO_2 and CH_4) fluxes in the Sacramento-San Joaquin Delta, Glob. Change Biol., 21, 750–765, 2015.

Koebsch, F., Glatzel, S., Hofmann, J., Forbrich, I., and Jurasinski, G.: CO_2 exchange of a temperate fen during the conversion from moderately rewetting to flooding, J. Geophys. Res.-Biogeo., 118, 940–950, doi:10.1002/jgrg.20069, 2013.

Köppen, W.: Das geographische System der Klimate, in: Handbuch der Klimatologie, Vol. IC, edited by: Köppen, W. and Geiger, R., Borntraeger, Berlin, C1–C44, 1936.

Koska, I., Succow, M., Clausnitzer, U., Timmermann, T., and Roth, S.: Vegetationskundliche Kennzeichnung von Mooren (topische Betrachtung), in: Landschaftsökologische Moorkunde, edited by: Succow, M. and Joosten, H., Schweizerbart, Stuttgart, 112–184, 2001.

Kottek, M., Grieser, J., Beck, C., Rudolf, B., and Rubel, F.: World map of the Köppen–Geiger climate classification up–dated, Meteorol. Z., 15, 259–263, 2006.

Kozulin, A., Tanovitskaya, N., and Vershitskaya, I.: Methodical Recommendations for Ecological Rehabilitation of Damaged Mires and Prevention of Disturbance to the Hydrological Regime of Mire Ecosystems in the Process of Drainage, Scientific and Practical Centre for Bio Resources, Institute for Nature Management of the National Academy of Sciences of Belarus, 2010.

Laine, A., Wilson, D., Kiely, G., and Byrne, K. A.: Methane flux dynamics in an Irish lowland blanket bog, Plant Soil, 299, 181–193, doi:10.1007/s11104-007-9374-6, 2007.

Leiber-Sauheitl, K., Fuß, R., Voigt, C., and Freibauer, A.: High CO_2 fluxes from grassland on histic Gleysol along soil carbon and drainage gradients, Biogeosciences, 11, 749–761, doi:10.5194/bg-11-749-2014, 2014.

Lloyd, J. and Taylor, J. A.: On the temperature dependence of soil respiration, Funct. Ecol., 8, 315–323, 1994.

Maksimenkov, M. V., Pugachevskij, A. V., and Rakovich, V. V.: Nauchnoe Obosnovanie povtornogo zabolachivaniya vyrabotannogo torfyanogo mestorozhdeniya “Bortenikha” (Scientific justification of rewetting of the cutaway peatland “Barcianicha”), The Forest Ministry of the Republic of Belarus, Minsk, 2006.

Michaelis, L. and Menten, M. L.: Die Kinetik der Invertinwirkung, Biochem. Z., 49, 333–369, 1913.

Minayeva, T., Sirin, A., and Bragg, O. (Eds.): A Quick Scan of Peatlands in Central and Eastern Europe, Wetlands International, Wageningen, 2009.

Minke, M., Augustin, J., Hagemann, U., and Joosten, H.: Similar methane fluxes measured by transparent and opaque chambers point at belowground connectivity of *Phragmites australis* beyond the chamber footprint, Aquat. Bot., 113, 63–71, 2014.

Moriasi, D. N., Arnold, J. G., Van Liew, M. W., Binger, R. L., Harmel, R. D., and Veith, T.: Model evaluation guidelines for systematic quantification of accuracy in water-shed simulations, T. ASABE, 50, 885–900, 2007.

Morrissey, L. A., Zobel, D. B., and Livingston, G. P.: Significance of stomatal control on methane release from *Carex*-dominated wetlands, Chemosphere, 26, 339–355, 1993.

Myhre, G., Shindell, D., Bréon, F.-M., Collins, W., Fuglestvedt, J., Huang, J., Koch, D., Lamarque, J.-F., Lee, D., Mendoza, B., Nakajima, T., Robock, A., Stephens, G., Takemura, T., and Zhang, H.: Anthropogenic and natural radiative forcing, in: Climate Change 2013: The Physical Science Basis, Contribution of Working Group I to the Fifth Assessment Report of the Intergovernmental Panel on Climate Change, edited by: Stocker, T. F., Qin, D., Plattner, G.-K., Tignor, M., Allen, S. K., Boschung, J., Nauels, A., Xia, Y., Bex, V., and Midgley, P. M., Cambridge University Press, Cambridge, UK, New York, NY, USA, 659–740, 2013.

Peet, R. K., Wentworth, T. R., and White, P. S.: A flexible, multipurpose method for recording vegetation composition and structure, Castanea, 63, 262–274, 1998.

Rinne, J., Riutta, T., Pihlatie, M., Aurela, M., Haapanala, S., Tuovinen, J.-P., and Tuittila, E.-S.: Annual cycle of methane emission from a boreal fen measured by the eddy covariance technique, Tellus B, 59, 449–457, 2007.

Rocha, A. V. and Goulden, M. L.: Large interannual CO_2 and energy exchange variability in a freshwater marsh under consistent environmental conditions, J. Geophys. Res., 113, G04019, doi:10.1029/2008JG000712, 2008.

Rocha, A. V., Potts, D. L., and Goulden, M. L.: Standing litter as a driver of interannual CO_2 exchange variability in a freshwater marsh, J. Geophys. Res., 113, G04020, doi:10.1029/2008JG000713, 2008.

Rothmaler, W.: Exkursionsflora von Deutschland: Kritischer Band (Flora of Germany), 9th edn., Spektrum, Heidelberg, Berlin, 2002.

Saarnio, S., Alm, J., Silvola, J., Lohila, A., Nykänen, H., and Martikainen, P. J.: Seasonal variation in CH_4 emissions and production and oxidation potentials at microsites on an oligotrophic pine fen, Oecologia, 110, 414–422, 1997.

Samaritani, E., Siegenthaler, A., Yli-Petäys, M., Buttler, A., Christin, P.-A., and Mitchell, E. A. D.: Seasonal net ecosystem carbon exchange of a regenerating cutaway bog: how long does it take to restore the C-sequestration function?, Restor. Ecol., 19, 480–489, doi:10.1111/j.1526-100X.2010.00662.x, 2011.

Scarton, F., Day, J. W., and Rismondo, A.: Above and belowground production of *Phragmites australis* in the Po Delta, Italy, Boll. Mus. civ. St. nat. Venezia, 49, 213–222, 1999.

Schierup, H. H.: Biomass and primary productivity in a *Phragmites communis* Trin. swamp in North Jutland, Denmark, Verh. Internat. Verein. Limnol., 20, 93–99, 1978, cited in: Westlake, D. F.: The primary productivity of water plants, in: Studies on Aquatic Vascular Plants, edited by: Symoens, J. J., Hooper, S. S., and Compère, P., Royal Botanical Society of Belgium, Bruessls, 165–180, 1982.

Schneider, J., Kutzbach, L., and Wilmking, M.: Carbon dioxide exchange fluxes of a boreal peatland over a complete growing season, Komi Republic, NW Russia, Biogeochemistry, 111, 485–513, 2012.

Schütz, H., Seiler, W., and Conrad, R.: Influence of soil temperature on methane emission from rice paddy fields, Biogeochemistry, 11, 11–95, 1990.

Soetaert, K., Hoffmann, M., Meire, P., Starink, M., Van Oevelen, D., Van Regenmortel, S., and Cox, T.: Modeling growth and carbon allocation in two reed beds (*Phragmites australis*) in the Scheldt estuary, Aquat. Bot., 79, 211–234, 2004.

Soini, P., Riutta, T., Yli-Petäys, M., and Vasander, H.: Comparison of vegetation and CO_2 dynamics between a restored cut-away peatland and a pristine fen: evaluation of the restoration success, Restor. Ecol., 18, 894–903, doi:10.1111/j.1526-100X.2009.00520.x, 2010.

Strachan, I. B., Nugent, K. A., Crombie, S., and Bonneville, M.-C.: Carbon dioxide and methane exchange at a cool-temperate freshwater marsh, Environ. Res. Lett., 10, 065006, doi:10.1088/1748-9326/10/6/065006, 2015.

Strack, M. and Zuback, Y. C. A.: Annual carbon balance of a peatland 10 yr following restoration, Biogeosciences, 10, 2885–2896, doi:10.5194/bg-10-2885-2013, 2013.

Tanneberger, F. and Wichtmann, W. (Eds.): Carbon Credits from Peatland Rewetting, Climate – Biodiversity – Land Use, Science, Policy, Implementation and Recommendations of a Pilot Project in Belarus, Schweizerbart, Stuttgart, 2011.

Tanovitskaya, N. and Kozulin, A.: Peatlands in Belarus, in: Carbon Credits from Peatland Rewetting, Climate – Biodiversity – Land Use, Science, Policy, Implementation and Recommendations of a Pilot Project in Belarus, edited by: Tanneberger, F. and Wichtmann, W., Schweizerbart, Stuttgart, 3–12, 2011.

Thiele, A., Edom, F., and Liashchynskaya, N.: Prediction of vegetation development with and without rewetting, in: Carbon Credits from Peatland Rewetting, Climate – Biodiversity – Land Use, Science, Policy, Implementation and Recommendations of a Pilot Project in Belarus, edited by: Tanneberger, F. and Wichtmann, W., Schweizerbart, Stuttgart, 42–52, 2011.

Tuittila, E.-S., Komulainen, V.-M., Vasander, H., and Laine, J.: Restored cut-away peatland as a sink for atmospheric CO_2, Oecologia, 120, 563–574, 1999.

Tuittila, E.-S., Komulainen, V.-M., Vasander, H., Nykänen, H., Martikainen, P. J., and Laine, J.: Methane dynamics of a restored cut-away peatland, Glob. Change Biol., 6, 569–581, 2000.

Van der Nat, F. J. and Middelburg, J. J.: Methane emission from tidal freshwater marshes, Biogeochemistry, 49, 103–121, 2000.

Vretare, V., Weisner, S. E. B., Strand, J. A., and Granéli, W.: Phenotypic plasticity in *Phragmites australis* as a functional response to water depth, Aquat. Bot., 69, 127–145, 2001.

Waddington, J. M. and Day, S. M.: Methane emissions from a peatland following restoration, J. Geophys. Res., 112, G03018, doi:10.1029/2007JG000400, 2007.

Westlake, D. F.: The primary productivity of water plants, in: Studies on Aquatic Vascular Plants, edited by: Symoens, J. J., Hooper, S. S., and Compère, P., Royal Botanical Society of Belgium, Bruessls, 165–180, 1982.

Wetlands International: Restoring Peatlands in Russia – For Fire Prevention and Climate Change Mitigation (PEATRUS), Seventh Progress Report, Submitted to KfW in August 2015.

Whalen, S. C.: Biogeochemistry of methane exchange between natural wetlands and the atmosphere, Environ. Eng. Sci., 22, 73–94, 2005.

Whiting, G. J. and Chanton, J. P.: Plant-dependent CH_4 emission in a subarctic Canadian fen, Global Biogeochem. Cy., 6, 225–231, 1992.

Whiting, G. J. and Chanton, J. P.: Primary production control of methane emission from wetlands, Nature, 367, 794–795, 1993.

Whiting, G. J. and Chanton, J. P.: Control of diurnal pattern of methane emission from aquatic macrophytes by gas transport mechanisms, Aquat. Bot., 54, 237–253, 1996.

Whiting, G. J. and Chanton, J. P.: Greenhouse carbon balance of wetlands: methane emission versus carbon sequestration, Tellus B, 53, 521–528, 2001.

Wickland, K.: Carbon gas exchange at a southern Rocky Mountain wetland, 1996–1998, Global Biogeochem. Cy., 15, 321–335, 2001.

Wilson, D., Tuittila, E.-S., Alm, J., Laine, J., Farrell, E. P., and Byrne, K. A.: Carbon dioxide dynamics of a restored maritime peatland, Ecoscience, 14, 71–80, 2007.

Wilson, D., Alm, J., Laine, J., Byrne, K. A., Farrell, E. P., and Tuittila, E.-S.: Rewetting of cutaway peatlands: are we re-creating hot spots of methane emissions?, Restor. Ecol., 17, 796–806, doi:10.1111/j.1526-100X.2008.00416.x, 2009.

Wilson, D., Farrell, C., Mueller, C., Hepp, S., and Renou-Wilson, F.: Rewetted industrial cutaway peatlands in western Ireland: a prime location for climate change mitigation?, MaP, 11, 1–22, 2013.

Yili-Petäys, M., Laine, J., Vasander, H., and Tuittila, E.-S.: Carbon gas exchange of a re-vegetated cut-away peatland five decades after abandonment, Boreal Environ. Res., 12, 177–190, 2007.

Zak, D., Reuter, H., Augustin, J., Shatwell, T., Barth, M., Gelbrecht, J., and McInnes, R. J.: Changes of the CO_2 and CH_4 production potential of rewetted fens in the perspective of temporal vegetation shifts, Biogeosciences, 12, 2455–2468, doi:10.5194/bg-12-2455-2015, 2015.

Zar, J. H.: Biostatistical Analysis, Prentice Hall, Upper Saddler River, 1999.

Zhou, L., Zhou, G., and Jia, Q.: Annual cycle of CO_2 exchange over a reed (*Phragmites australis*) wetland in Northeast China, Aquat. Bot., 91, 91–98, 2009.

Title Page
Abstract Introduction
Conclusions References
Tables Figures
◀| |▶
◀ ▶
Back Close
Full Screen / Esc
Printer-friendly Version
Interactive Discussion

BGD
12, 17393–17452, 2015

Title Page
Abstract | Introduction
Conclusions | References
Tables | Figures
◀| |▶
◀ ▶
Back | Close
Full Screen / Esc
Printer-friendly Version
Interactive Discussion

Table 1. Site characteristics.

Site	Plot	Annual, summer, winter water level[a] (median, cm above surface)		Above Ground biomass[b] ($\mathrm{g\,C\,m^{-2}}$)	Surface peat				Profile description, top down[e]
		1st year	2nd year		pH[c]	C[d] (%)	N[d] (%)	C/N ratio	
BA *Eriophorum–Carex*	I	−2, −3, −2	−2, −3, 0	156	6.1	40.3	2.2	18.3	0–9 radicel peat (H6), 9–14 silty gyttja, 14–43 radicel peat (H4, H3), 43–119 brown moss peat (H3, H4), below: middle sand
	II	−3, −4, −3	−3, −4, −1	98	6.1	43.2	2.3	18.7	
	III	−5, −5, −4	−5, −5, −3	97	6.4	43.2	2.3	18.6	
BA *Carex–Equisetum*	I	9, 8, 9	9, 8, 10	61	6.1	42.8	2.4	17.7	0–15 radicel peat (H6), 15–30 radicel brown moss peat (H3), 30–34 *Alnus* peat (H4), 34–85 brown moss peat (H3), 85–95 clayey gyttja and coarse sand, below: fine sand
	II	7, 7, 7	7, 7, 9	73	6.1	43.1	2.5	17.0	
	III	8, 7, 8	8, 7, 10	31	6.1	43.0	2.8	15.6	
BA *Phragmites–Carex*	I	13, 13, 14	13, 13, 15	221	6.0	44.1	2.8	16.0	0–13 lost, 13–40 radicel peat (H5/H4), 40–67 brown moss peat (H3, H4), below: gravel
	II	13, 13, 14	13, 13, 15	379	6.1	43.5	2.8	16.3	
	III	16, 15, 16	16, 15, 17	287	6.1	43.7	2.4	18.0	
GK *Typha–Hydrocharis*	I	12, 7, 15	4, 1, 4	295	5.6	45.0	3.0	14.8	0–20 lost, 20–30 radicel peat (H5), 30–55 very highly decomposed peat with radicels (H8), 55–90 radicel peat with *Phragmites* (H5, H3), 103–113 woody radicel peat with *Phragmites* (H4), 90–103 brownmoss–radicel peat (H3), 113–140 radicel peat with *Phragmites* and brown mosses (H4), 140–150 organogyttja, below: sand
	II	12, 7, 15	4, 1, 4	142	5.5	39.4	2.7	14.5	
	III	7, 2, 10	−2, −4, −1	339	5.6	39.7	2.7	15.0	
GK *Carex–Lysimachia*	I	8, 4, 10	2, 0, 2	305	6.5	44.6	3.1	14.5	
	II	13, 9, 15	7, 5, 7	195	6.5	44.0	2.3	18.8	
	III	10, 7, 12	4, 2, 4	358	6.4	45.0	2.4	18.5	
GK *Phragmites–Lemna*	I	108, 90, 118	78, 69, 79	725	5.7	32.4	2.2	14.7	0–10 very highly decomposed peat with radicels (H8), 10–100 radicel peat with *Phragmites* (H4, H5), 100–170 radicel peat (H5), 170–185 organogyttja, below: sand
	II	107, 89, 117	77, 68, 78	502	5.7	39.1	2.5	15.6	
	III	98, 80, 108	67, 59, 69	531	5.8	39.8	2.6	15.2	

[a] Summer = June–August, winter = December–February.

[b] Harvest at Barcianicha (first three sites) 29 October 2012, and at Giel’čykaŭ Kašyl’ (last three sites) 11 September 2012.

[c] pH (KCL) mean of three samples.

[d] Total carbon and nitrogen content, one sample.

[e] von Post peat decomposition scale: H3 very slightly, H4 slightly, H5 moderately, H6 moderately highly, H8 very highly decomposed peat.

Table 2. Plant species cover of GHG measuring plots in summer 2010 and 2012.

	BA *Eriophorum–Carex*						BA *Carex–Equisetum*						BA *Phragmites–Carex*					
	2010			2012			2010			2012			2010			2012		
species	I	II	III	I	II	III	I	II	III	I	II	III	I	II	III	I	II	III
Eriophorum angustifolium	6	6	7	6	6	6												
Marantia polymorpha	3	2	2						2									
Dicranella cerviculata	3	2	2	3	4	4		6	2									
Juncus cf.*compressus*		1		3	2	2	2	2		2	2	2						
Utricularia intermedia											2	2	7	6	7			
Chara spec.										2		3				1		
green algae												4				2		
Phragmites australis											1		7	8	6	8	8	8
Dicranella heteromalla													2	2	2			
Carex rostrata	2	2	3	2	2	2	7	7	6	7	6	6	3	3	3	3	3	3
Equisetum fluviatile	2			2	2		2	2	2	2	2	2	1	1	1	1		1
Salix cinerea	1	1		1			1	1	1	1			1		4	1		
Drepanocladus aduncus			2										5			2		4

	GK *Carex–Lysimachia*						GK *Typha–Hydrocharis*						GK *Phragmites–Lemna*					
	2010			2012			2010			2012			2010			2012		
species	I	II	III	I	II	III	I	II	III	I	II	III	I	II	III	I	II	III
Thelypteris palustris	4					6												
Calamagrostis neglecta	4					2												
Carex elata	2	5	6	8	5	2			7			8						
Carex vesicaria	7	2		3	6	2	2	3		5	5							
Typha latifolia	6	7	6		4	4	6	7	3	6	3	4						
Galium palustre	2	2	2	2	2	2				2	2	2						
Cardamine amara	2	2	1	2	2				1	2	1	2						
Lycopus europeus		2		2	2	2			1		1	1						
Lysimachia thyrsiflora	1	2	2	3	2	2				2	4	2						
Lemna trisulca							2				2			1		2	2	2
Phragmites australis													7	7	8	9	7	8
Stratiotes aloides													1	6			5	2
Drepanocladus aduncus	2	5	2	6	8	3	3	2	2	8	3	7	2			2		2
Hydrocharis morsus–ranae				2	3	2	3	3	2	4	6	3	3	5	4	5	8	6
Lemna minor					2	2	2	1		2	2	2	1	1		2		

Vegetation types of sites studied in Barcianicha: *Eriophorum angustifolium–Carex rostrata*–reed (BA *Eriophorum–Carex*), *Carex rostrata–Equisetum fluviatile*–reed (BA *Carex–Equisetum*), *Phragmites australis–Carex rostrata*–reed (BA *Phragmites–Carex*), and Giel'čykaŭ Kašyl': *Carex elata–Lysimachia thyrsiflora*–reed (GK *Carex–Lysimachia*), *Typha latifolia–Hydrocharis morsus–ranae*–reed (GK *Typha–Hydrocharis*), *Phragmites australis–Lemna trisulca*–reed (GK *Phragmites–Lemna*). Plant cover scale according to Peet et al. (1998): Class 1 = very few individuals, 2 = cover of 0–1 %, 3 = 1–2 %, 4 = 2–5 %, 5 = 5–10 %, 6 = 10–25 %, 7 = 25–50 %, 8 = 50–75 %, 9 = 75–95 %, 10≧95 %. Species not exceeding cover class 2 are only shown if they meet class 2 in more than two relevés.

Table 3. Annual fluxes of CO_2, CH_4, and Carbon (C balance = NEE + CH_4 emissions) with 90 % confidence intervals.

Site	Year	R_{eco} ($g\,CO_2-C\,m^{-2}\,yr^{-1}$)	GPP ($g\,CO_2-C\,m^{-2}\,yr^{-1}$)	NEE ($g\,CO_2-C\,m^{-2}\,yr^{-1}$)	CH_4 emissions ($g\,CH_4-C\,m^{-2}\,yr^{-1}$)	C balance ($g\,C\,m^{-2}\,yr^{-1}$)
BA *Eriophorum–Carex*	1	364 (339 to 396)	−449 (−512 to −407)	−86 (−130 to −38)	10 (9 to 13)	−75 (−114 to −30)
	2	406 (368 to 458)	−413 (−449 to −376)	−7 (−49 to 21)	11 (10 to 14)	4 (−35 to 30)
BA *Carex–Equisetum*	1	232 (196 to 262)	−320 (−361 to −279)	−88 (−114 to −68)	17 (13 to 22)	−71 (−92 to −56)
	2	327 (282 to 371)	−302 (−334 to −281)	24 (−6 to 55)	13 (9 to 16)	37 (8 to 66)
BA *Phragmites–Carex*	1	614 (478 to 737)	−1141 (−1595 to −888)	−528 (−933 to −194)	42 (28 to 58)	−486 (−873 to −156)
	2	706 (568 to 842)	−1035 (−1134 to −949)	−329 (−431 to −220)	36 (22 to 52)	−293 (−377 to −205)
GK *Typha–Hydrocharis*	1	921 (841 to 982)	−771 (−842 to −665)	151 (41 to 300)	60 (47 to 77)	210 (111 to 360)
	2	973 (818 to 1156)	−1086 (−1476 to −862)	−113 (−418 to 66)	68 (52 to 92)	−45 (−343 to 142)
GK *Carex–Lysimachia*	1	1105 (1007 to 1207)	−940 (−1081 to −774)	166 (66 to 252)	86 (63 to 121)	252 (145 to 356)
	2	1270 (1221 to 1362)	−1054 (−1243 to −789)	216 (48 to 470)	85 (59 to 142)	301 (137 to 552)
GK *Phragmites–Lemna*	1	936 (733 to 1200)	−1547 (−1726 to −1386)	−611 (−819 to −450)	100 (48 to 147)	−516 (−747 to −349)
	2	1092 (937 to 1210)	−2267 (−2733 to −1843)	−1175 (−1567 to −690)	101 (61 to 177)	−1074 (−1453 to −565)

Uncertainties on the site level include the uncertainties of the plot models and the spatial heterogeneity. They were calculated by pooling the plot specific annual models derived by error calculation. Different CO_2 balances of APPROACH ONE and APPROACH TWO were accounted for by adding the differences randomly to 50 % of the respective annual values derived by error calculation with APPROACH ONE. To derive uncertainties of C balances the annual models of NEE and CH_4 derived by plot-wise error calculation were summarized and combined site-wise.

Table 4. Inter-annual and small scale spatial variability of net CO_2 and methane emissions.

Site	Inter-annual variability[a]		Small scale spatial variability[b]	
	NEE ($g\,CO_2-C\,m^{-2}\,yr^{-1}$)	CH_4 emissions ($g\,CH_4-C\,m^{-2}\,yr^{-1}$)	NEE ($g\,CO_2-C\,m^{-2}\,yr^{-1}$)	CH_4 emissions ($g\,CH_4-C\,m^{-2}\,yr^{-1}$)
BA *Eriophorum–Carex*	39 ± 12	0.5 ± 0.0	16 ± 13	0.5 ± 0.2
BA *Carex–Equisetum*	56 ± 8	2.3 ± 0.5	9 ± 5	1.4 ± 0.7
BA *Phragmites–Carex*	110 ± 113	3.0 ± 3.6	125 ± 140	6.4 ± 2.7
GK *Typha–Hydrocharis*	132 ± 64	4.2 ± 2.9	121 ± 66	3.2 ± 3.2
GK *Carex–Lysimachia*	74 ± 56	1.2 ± 0.9	95 ± 73	10.9 ± 8.3
GK *Phragmites–Lemna*	282 ± 177	11.6 ± 2.8	187 ± 153	24.2 ± 10.0

Given are means ± standard deviations, $n = 6$.

[a] Inter-annual variability, calculated as the mean of the absolute differences between annual plot emissions and two years plot mean.

[b] Small scale spatial variability, calculated as the mean of the absolute differences between annual plot emissions and annual site emissions.

Table 5. GHG balances based on the global warming potentials of CO_2, CH_4 and N_2O for a time horizon of 100 yr (GWP_{100} of CO_2 = 1, of CH_4 = 28 and of N_2O = 265 CO_2-equivalents, Myhre et al., 2013) with 90 % confidence intervals.

Site	Year	CO_2 balance ($t\,CO_2\,eq\,ha^{-1}\,yr^{-1}$)	CH_4 balance ($t\,CO_2\,eq\,ha^{-1}\,yr^{-1}$)	N_2O balance ($t\,CO_2\,eq\,ha^{-1}\,yr^{-1}$)	GHG balance ($t\,CO_2\,eq\,ha^{-1}\,yr^{-1}$)
BA *Eriophorum–Carex*	1	−3.1 (−4.8 to −1.4)	3.8 (2.9 to 5.0)	−0.1 (−0.8 to 0.8)	0.5 (−1.4 to 3.1)
	2	−0.3 (−1.8 to 0.8)	4.2 (3.6 to 5.1)	0.2 (−0.2 to 0.8)	4.1 (2.3 to 6.0)
BA *Carex–Equisetum*	1	−3.2 (−3.2 to −2.5)	6.4 (5.0 to 8.0)	−0.1 (−0.7 to 0.5)	3.1 (1.9 to 5.0)
	2	0.9 (−0.2 to 2.1)	4.7 (3.2 to 6.1)	−0.3 (−0.9 to 0.2)	5.3 (3.3 to 7.3)
BA *Phragmites–Carex*	1	−19.4 (−34.2 to −7.1)	15.6 (10.4 to 21.6)	−0.3 (−2.9 to 3.0)	−4.1 (−16.9 to 11.9)
	2	−12.1 (−15.8 to −8.1)	13.3 (8.4 to 19.4)	−0.6 (−3.6 to 2.0)	0.7 (−6.5 to 6.6)
GK *Typha–Hydrocharis*	1	5.5 (1.5 to 11.0)	22.3 (17.4 to 28.6)	0.6 (−1.7 to 2.7)	28.5 (21.5 to 38.9)
	2	−4.2 (−15.3 to 2.4)	25.5 (19.3 to 34.4)	0.4 (−0.7 to 1.5)	21.7 (7.6 to 36.1)
GK *Carex–Lysimachia*	1	6.1 (2.4 to 9.2)	32.3 (23.6 to 45.5)	−0.1 (−2.1 to 1.8)	38.2 (27.8 to 53.7)
	2	7.9 (1.8 to 17.2)	31.6 (22.2 to 53.1)	0.4 (−0.8 to 1.9)	39.9 (25.8 to 60.7)
GK *Phragmites–Lemna*	1	−22.4 (−30.0 to −16.5)	35.7 (18.0 to 54.7)	0.6 (−2.4 to 3.8)	13.9 (−10.6 to 36.0)
	2	−43.1 (−57.5 to −25.3)	37.7 (22.9 to 66.2)	0.0 (−3.5 to 3.4)	−5.4 (−29.2 to 40.0)

Confidence intervals include the uncertainties of the plot models and the spatial heterogeneity. To derive uncertainties of GHG balances the annual models of CO_2 (NEE), CH_4 and N_2O derived by plot-wise error calculation were summarized and combined site-wise.

Table 6. Estimation of net primary production (NPP), heterotrophic (R_h) and autotrophic respiration (R_a) from the *Phragmites australis* sites.

Site	Year	GPP ($g CO_2-C m^{-2} yr^{-1}$)	NEE ($g CO_2-C m^{-2} yr^{-1}$)	AGB, green ($g C m^{-2}$)[a]	Assumed ratio BG NPP/AG NPP[b]	NPP ($g C m^{-2} yr^{-1}$)[c]	R_h ($g CO_2-C m^{-2} yr^{-1}$)[d]	R_a ($g CO_2-C m^{-2} yr^{-1}$)[e]	R_a/[GPP]
BA *Phragmites–Carex*	1	−1141	−528	260	1.4	624	96	517	0.45
	2	−1035	−329	169	1.4	406	77	629	0.61
GK *Phragmites–Lemna*	1	−1547	−611	322	1.2	707	96	840	0.54
	2	−2267	−1175	586	1.2	1289	114	978	0.43

[a] Green above ground biomass (AGB) present at end of the first measuring year was estimated for each GHG-plot from biomass harvest at three to four sample plots (40 cm × 40 cm) close to collars accordingly to the share of green vs. dead culms. At the end of the second year green AGB of the plots was calculated from the plot harvest (Table 1) accordingly to the share of green vs. dead culms.

[b] Green AGB was assumed to equal above ground net primary production (AG NPP), although this may underestimate NPP by about 10 % (Westlake, 1982). Reported below ground net primary production (BG NPP) to AG NPP ratios range from 0.34–2.58 (Westlake, 1982; Scarton et al., 1999; Soetaert et al., 2004; Asaeda et al., 2006). We used the estimate of 1.4 from reeds in North Jutland (Schierup, 1978; cited in Westlake, 1982) for BA *Phragmites–Carex* and a lower ratio (1.2) for GK *Phragmites–Lemna*, because below ground biomass allocation of *Phragmites australis* was found to be proportionally less in deep (70 or 75 cm), compared to shallow (20 or 5 cm) water (Vretare et al., 2001).

[c] Net primary production (NPP) = AG NPP + BG NPP.

[d] Heterotrophic respiration (R_h) = NPP − [NEE].

[e] Autotrophic respiration (R_a) = [GPP] − NPP.

Table 7. Net annual CO_2 and CH_4 emissions from temperate wetlands with vegetation comparable to Barcianicha’ and Giel’čykaŭ Kašyl’.

Location, climate[a]	Site description, method[b]	Dominant plant species	Study years	water level[c] (cm above surface)	NEE[d] ($g\,CO_2-C\,m^{-2}\,yr^{-1}$)	CH_4 emissions[d] ($g\,CH_4-C\,m^{-2}\,yr^{-1}$)	Reference
Oweninny bog, Ireland, 54.12° N 9.58° W (Cfb)	cutover blanket bog with oligotrophic, acid peat, rewetted 2003 (ch)	*Eriophorum angustifolium*	2009 to 2011	7 ± 1	−348 ± 222	5.3 ± 0.1	Wilson et al. (2013)
Turraun, Ireland, 53.28° N 7.75° W (Cfb)	cutover bog with slightly acidic peat and calcareous subsoil, rewetted 1991 (ch)	*E. angustifolium–Carex rostrata* *Typha latifolia*	2002 to 2003 2002 to 2003	5, −6.3 7, 0.3	163, 408 266, 451	3.2, 2.4 29.1, 21.6	Wilson et al. (2007, 2009)
Trebel valley mire complex, NE Germany, 54.10° N 12.73° E (Cfb)	former fen grassland, rewetted 1997 (ch)	*Phragmites australis* *T. latifolia* *C. acutiformis*	2011/12 to 2012/13	−9, −19 6, −4 5, −3	−83, 68 −43, 94 −3, 81	11, 1 10, 3 47, 3	Günther et al. (2014)
Mokre’Louky, Czech Republic, 49.02° N 14.77° E (Cfb)	eutrophicated sedge fen (ec)	*C. acuta*	2006 to 2008	−20 to 10	−199 ± 66		Dušek et al. (2012)
Vejlerne Nature Reserve, Denmark, 56.93° N 9.05° E (Cfb)	brackish wetland (ch, 10 occasions, two years)	*P. australis*		summer – to winter +	−552	48	Brix et al. (2001)
Horstermeer, Netherlands, 52.14° N 5.04° E (Cfb)	land along the ditches of a former fen grassland, rewetted about 1995 (ch)	*P. australis–T. latifoliar*	2006	−2 to 5		87.6	Hendriks et al. (2007)
Virginia, USA, 37° N 76.5° W (Cfb)	freshwater marsh (ch)	*T. latifolia*	1992/93	5 to 20	−896	81.6	Whiting and Chanton (2001)
Florida, USA, 30.5° N 84.25° W (Cfa)	lake shore (ch)	*T. latifolia*	1992 to 1993	5 to 20	−978, −1139	51.6, 72.0	Whiting and Chanton (2001)
San Joaquin Freshwater Marsh, California, USA, 33.66° N 117.85° W (Csb)	freshwater marsh (ec)	*T. latifolia*	1999 to 2003	summer – to winter +	136 ± 363		Rocha and Goulden (2008)
Sacramento-San Joaquin Delta, California, USA, 1st site: 38.05° N 121.77° W, 2nd site: 38.11° N 121.65° W (Csa)	former fen pasture, rewetted 2010 (ec) former agricultural fen, rewetted 1997 (ec)	*T. spp., Schoenoplectus acutus*	2012/13	107 26	−368 −397	53 38.7	Knox et al. (2015)
Mer Bleue, Ontario, Canada, 45.4° N 75.5° W (Dfb)	freshwater marsh (ec–NEE, ch–CH_4)	*T. angustifolia*	2005 to 2009	at surface	−224 ± 54	127 ± 19	Strachan et al. (2015)

Table 7. Continued.

Location, climate[a]	Site description, method[b]	Dominant plant species	Study years	water level[c] (cm above surface)	NEE[d] ($\text{g CO}_2-\text{C m}^{-2}\text{ yr}^{-1}$)	CH_4 emissions[d] ($\text{g CH}_4-\text{C m}^{-2}\text{ yr}^{-1}$)	Reference
Ballards Marsh, Nebraska, USA, 42.87° N 100.55° W (Dfa)	freshwater marsh, 10 to 30 cm litter (ec)	*P. australis*	1994	40 to 60		60	Kim et al. (1998)
Winous Point, Lake Erie, Ohio, USA, 41.47° N 83° W (Dfa)	freshwater marsh, 20 cm organic layer (ec)	*T. angustifolia–Nymphaea odorata*	2011 to 2013	20 to 60	65 ± 92	50.8 ± 6.9	Chu et al. (2015)
Lake Vesijärvi, S Finland, 61.08° N 25.50° E (Dfc)	inundated peatland on the shore of an eutrophic lake (ch)	*P. australis*	1997 to 1999	10 to 20		33 ± 13.5	Kankaala et al. (2004)
		P. australis	1997 to 1999	30 to 70		122.3 ± 56.5	
Loch Vale watershed, Colorado, USA, 40.29° N 105.66° W (Dfc)	pristine sedge fen (ch)	*C. aquatilis*	1996 to 1998	water saturated	81 ± 4	31.2 ± 2.1	Wickland et al. (2001)
Panjin Wetland, Liaoning Province, NE China, 41.13° N 121.90° E (Dwa)	freshwater tidal wetland with silty clay (ec)	*P. australis*	2005	vol. SWC 3 to 46 %	−65		Zhou et al. (2009)

[a] climate type after Köppen and Geiger (Kottek et al., 2006): Cfb – Warm temperate, fully humid, warm summer; Cfa – Warm temperate, fully humid, hot summer; Csb – Warm temperate with dry and warm summer; Csa – Warm temperate with dry and hot summer; Dfb – Snow climate, fully humid, warm summer; Dfa – Snow climate, fully humid, hot summer; Dfc – Snow climate, fully humid, cool summer and cold winter; Dwa – Snow climate with dry winter and hot summer.

[b] ch – chamber method, ec – eddy covariance method.

[c] Annual water level (listed for one or two years, but given as mean ± standard deviation when three or more years) or water level range (water level of dry to water level of wet season).

[d] Annual NEE and methane emissions, listed for one or two years, but given as mean ± standard deviation when three or more years.

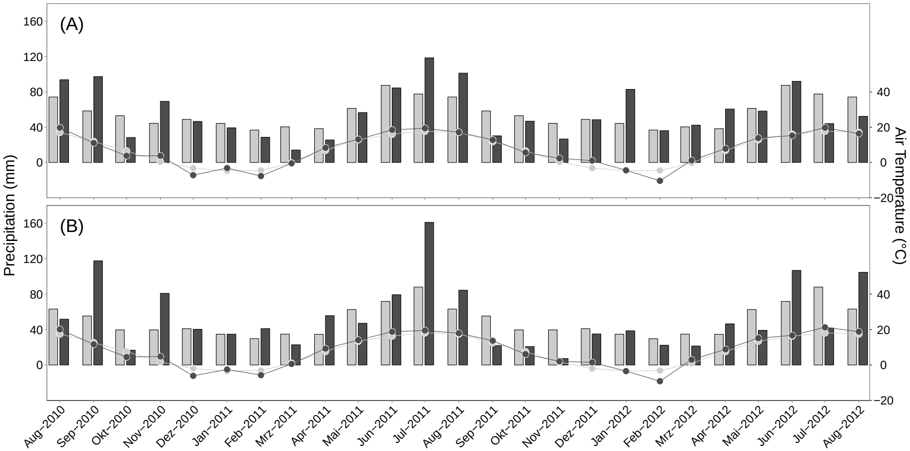

Figure 1. Cumulative monthly precipitation (bars) and average monthly air temperatures (dots) for Barcianicha **(a)** and Giel’čykaŭ Kašyl’ **(b)**. Actual temperatures (black) were measured in **(a)** Višnieva, 5.6 km NW of Barcianicha, and **(b)** Z’dzitava, 6.3 km NE of Giel’čykaŭ Kašyl’. Actual precipitation data (black) and 30 year averages (1979–2008) of temperatures and precipitation (grey) are from meteorological stations of “Gidrometcentr” in **(a)** Valožyn, 15 km E of Barcianicha, and **(b)** Pružany, 54 km WNW of Giel’čykaŭ Kašyl’.

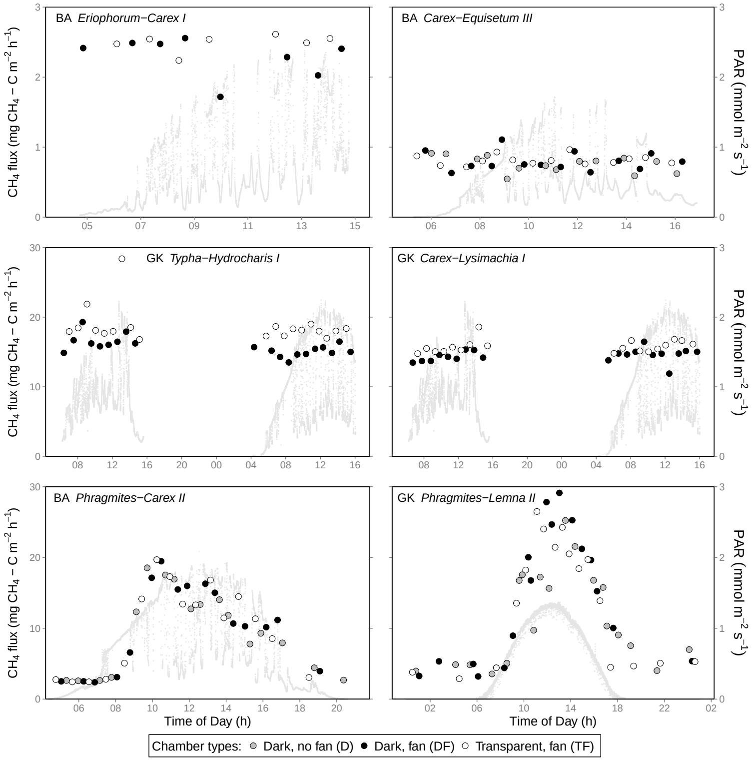

Figure 2. Diurnal variation of methane emissions, measured with different chamber types, and outside PAR, at BA *Eriophorum–Carex* (plot I, 18 July 2012), BA *Carex–Equisetum* (plot III, 16 September 2012), BA *Phragmites–Carex* (plot II, 8 August 2012), GK *Typha–Hydrocharis* and GK *Carex–Lysimachia* (both plot I, 12 and 13 July 2012), and GK *Phragmites–Lemna* (plot II, 21 September 2011). Data of BA *Phragmites–Carex* and GK *Phragmites–Lemna* are from Minke et al. (2014).

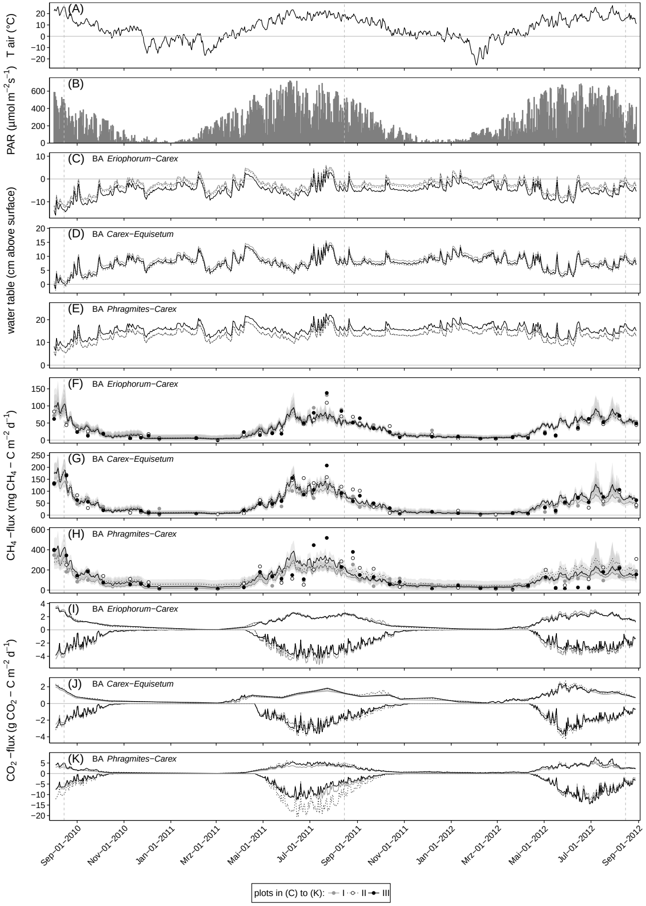

Figure 3. Mean daily air temperature **(a)** and mean daily PAR **(b)** at Višnieva, and mean daily water table position **(c–e)**, mean daily measured (points) and modeled (lines) CH$_4$ fluxes **(f–h)**, and mean daily modeled (APPROACH ONE) GPP, and R_{eco} **(i–k)** of Barcianicha sites.

Title Page
Abstract
Introduction
Conclusions
References
Tables
Figures
◀
▶
Back
Close
Full Screen / Esc
Printer-friendly Version
Interactive Discussion

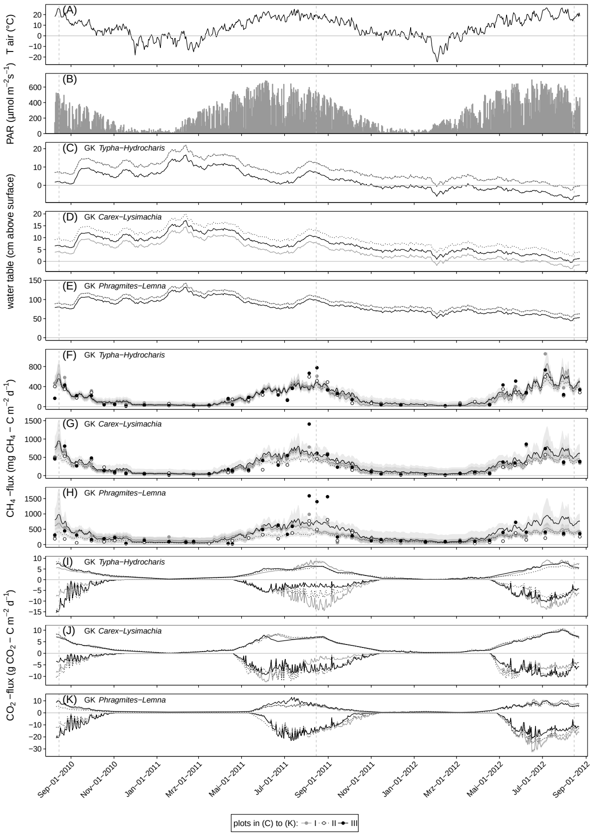

Figure 4. Mean daily air temperature **(a)** and mean daily PAR **(b)** at Z’dzitava, and mean daily water table position **(c–e)**, mean daily measured (points, for F and G multiplied with 1.2) and modeled (lines) CH$_4$ fluxes **(f–h)**, and mean daily modeled (APPROACH ONE) GPP and R_{eco} **(i–k)** of Giel’čykaŭ Kašyl’ sites.

Title Page
Abstract | Introduction
Conclusions | References
Tables | Figures
◀| | |▶
◀ | ▶
Back | Close
Full Screen / Esc
Printer-friendly Version
Interactive Discussion

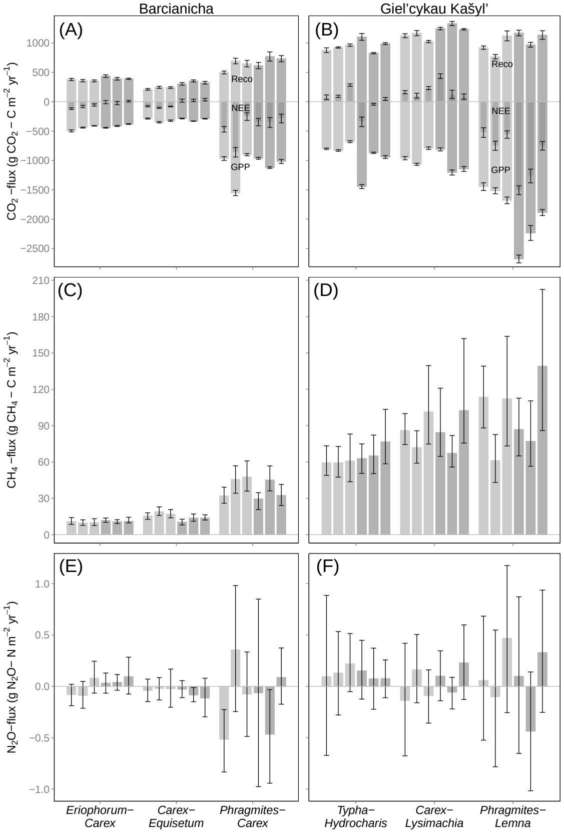

Figure 5. Annual CO_2 (NEE, R_{eco}, GPP), CH_4 and N_2O fluxes at Barcianicha **(a, c, e)** and Giel'čykaŭ Kašyl' **(b, d, f)**. Uncertainties for CO_2 fluxes are 50 % of the difference between both modelling approaches plus the 90 % confidence intervals of APPROACH ONE. Uncertainties for CH_4 represent 90 % confidence intervals of the models, but for N_2O only 90 % CI of the measured N_2O fluxes. Light grey = 1st year, darker grey = 2nd year. Plots are ordered I, II, III.

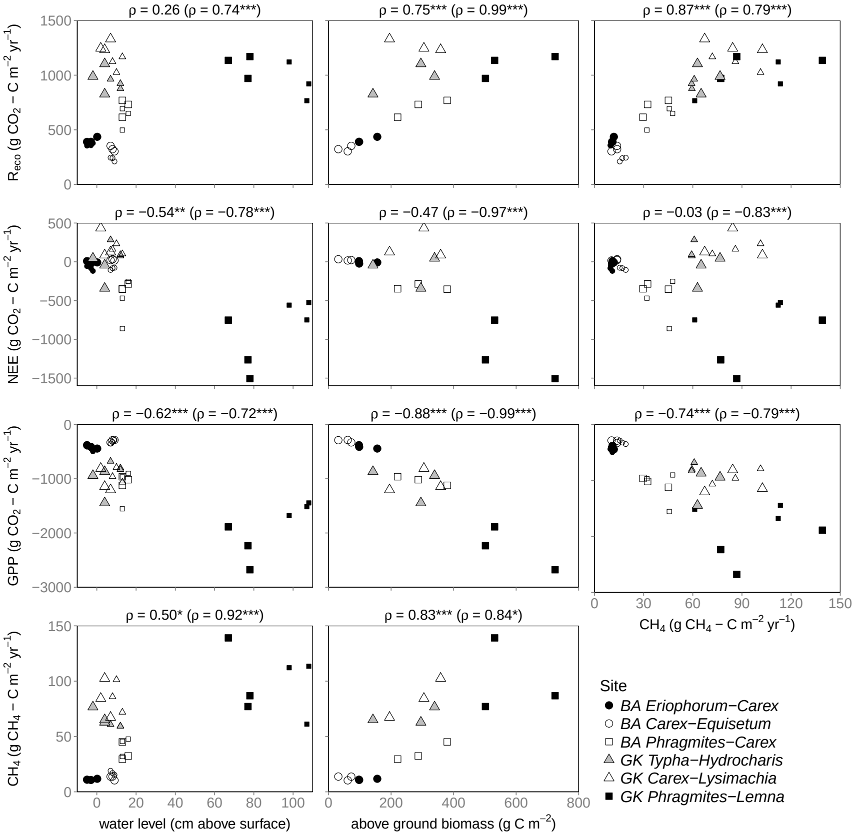

Figure 6. Correlations among annual NEE, R_{eco}, GPP, CH_4 emissions, median annual water levels (both years for all plots, $n = 36$), and above ground biomass carbon (second year for all plots, $n = 18$). Spearman's ρ significant at $'$ $P \leq 0.05$; * $P \leq 0.01$; ** $P \leq 0.001$; *** $P \leq 0.0001$. Spearman's ρ in brackets without GK *Typha–Hydrocharis* and GK *Carex–Lysimachia* ($n = 30$ for correlations among water levels and fluxes; $n = 15$ for correlations among biomass and fluxes). Small symbols indicate first year, large symbols second year.